

# Timelike transitions in an atom by a mirror in light cone and Kruskal-Szekeres regions: a status of quantum equivalence

Subhajit Barman,<sup>1,\*</sup> Pradeep Kumar Kumawat,<sup>2,†</sup> and Bibhas Ranjan Majhi<sup>2,‡</sup>

<sup>1</sup>*Centre for Strings, Gravitation and Cosmology, Department of Physics,  
Indian Institute of Technology Madras, Chennai 600036, India*

<sup>2</sup>*Department of Physics, Indian Institute of Technology Guwahati, Guwahati 781039, Assam, India*  
(Dated: March 4, 2025)

We investigate the timelike transitions in a two-level atom in the presence of an infinite reflecting mirror in the future-past light cone regions of a Minkowski spacetime as well as in the region interior of a  $(1+1)$  dimensional Schwarzschild black hole. In particular, when considering the light cone regions, two specific scenarios are dealt with – (i) a static mirror is synchronized with Minkowski time while the static atom is using a frame in the light cone, (ii) a static atom is using Minkowski time, and the mirror is using the light cone frame. Analogous scenarios in the black hole spacetime are – the static mirror uses future Kruskal frame while the static atom uses the Schwarzschild coordinates, defined inside the black hole, and vice-versa. The calculations, depending upon the frame of the atom, are respectively done within the light cone, Minkowski, Schwarzschild, and Kruskal time-interaction pictures. In all of these scenarios, we observe that the excitation probabilities contain a thermal factor and are periodic on the separation between the atom and the mirror, contrasting the uniform acceleration scenario. The above two scenarios in  $(1+1)$  dimensional Minkowski-light cone regions appear to be the same when we equate the field and atomic frequencies. However, the same is not true when we consider the  $(3+1)$  dimensional Minkowski-light cone or the Schwarzschild interior regions. We also estimate the de-excitation probabilities and encounter similar situations. However, we observe that the ratio between the excitation and corresponding de-excitation probabilities resembles the classical equivalence in motion at the quantum level. The excitation to de-excitation ratios (EDRs) corresponding to analogous scenarios are equal for equal atomic and field frequencies. This bolsters our earlier proposal on the relevance of EDRs in the context of the equivalence principle.

## I. INTRODUCTION

The phenomenon of spontaneous creation of quantum particles occurs in various instances, like the Schwinger effect, Hawking radiation, Unruh effect, Casimir effect, etc. [1]. Among these, the Unruh effect bears a special role in understanding gravity at the quantum regime. Einstein's equivalence principle (EEP) [2] – the trajectories of a particle under gravity are indistinguishable locally from those for a free particle viewed with respect to an accelerated frame and therefore, locally, the gravitational field is indistinguishable from a suitably chosen accelerated frame – motivates the study of physics in the accelerated frame to understand the local features of gravity. On the other hand, weak equivalence principle (WEP) [2] – the equation of motion of a particle is independent of spacetime curvature and so it is given by geodesics – holds a key nerve to connect non-inertial frame without gravity with a static frame under gravity, as far as motion is concerned. In fact, one finds that an accelerated frame in Minkowski spacetime is equivalent to a stationary observer in black hole spacetime, while a Minkowski frame is equivalent to a freely falling observer in black hole spacetime. However, the validity of these equivalences at the quantum level is still a questionable one (see [2, 3] for various investigations). In this regard, the Unruh effect appears to be a very important phenomenon to test the validity of these aforesaid principles.

Rindler observer sees a sea of particles in the Minkowski vacuum, celebrated as Unruh effect [4]; in fact, one finds  $\langle O_M | \hat{N}_R | 0_M \rangle$  is given by thermal distribution. Due to the symmetry in the relative motions (manifestation of EEP) among two frames (Minkowski and Rindler), one expects that  $\langle O_M | \hat{N}_R | 0_M \rangle \equiv \langle O_R | \hat{N}_M | 0_R \rangle$ . Here  $|0_M\rangle$  ( $|0_R\rangle$ ) stands for Minkowski (Rindler) vacuum while  $\hat{N}_R$  ( $\hat{N}_M$ ) signifies the number operator in Rindler (Minkowski) frame. The validity of this has been successfully demonstrated in the literature (see e.g. [5]) in free (i.e. without boundary, like a mirror) spacetime. The excitation probability of an atom (modelled as Unruh-DeWitt detector) by

---

\*Electronic address: subhajit.barman@physics.iitm.ac.in

†Electronic address: pradeep.kumawat@iitg.ac.in

‡Electronic address: bibhas.majhi@iitg.ac.in

the virtual transition is one of the possible observables of this phenomenon, known as the detector's response [6]. Two situations can arise. The transition of the accelerated atom which can be described as – in the accelerated frame the atom is excited by absorbing Rindler particle [4, 7] or the inertial observer describes the same event as acceleration radiation by emitting Minkowski particle [7, 8]. Due to the symmetry in the relative motions among these two frames, the static atom can be excited. Likewise, this can be considered as the excitation of the static atom by absorbing Minkowski particles with respect to the inertial observer or equivalently in the Rindler frame such can be viewed as the acceleration radiation due to the emission of Rindler particles. Although these two situations are phenomenologically different [7], apparently they follow a symmetry among them to validate the EEP at the quantum regime (see also [9]). However, it is always necessary to test the same to obtain a concrete conclusion. Moreover, the number operator calculation can not illuminate this as physically the detector's response is a different phenomenon from the particle production event.

To illuminate the area an analytic investigation of the transition probability of a two-level atom has been done in [7] by considering two situations – (I) a mirror is static in Minkowski spacetime while the atom is uniformly accelerating and (II) the mirror is accelerating uniformly when the atom is static on Minkowski frame. Note that at the classical level, both situations are identical as far as the relative motions between the atom and mirror are concerned. The investigation in [7] concludes that the transition probabilities are identical when the photon and atom frequencies are the same. Moreover, the thermal factors in both situations contain symmetry under the exchange of photon and atom frequencies. This is regarded as a manifestation of EEP at the quantum level. Additionally, as a manifestation of WEP, case-I should be identical to the excitation of the static atom when the mirror is freely falling in the black hole spacetime with the surface gravity of the black hole identified as the acceleration parameter. Also, case II must coincide with the transition of the atom, which is freely falling with the mirror static in black hole spacetime. Consequently, two situations for black hole spacetime must contain the aforesaid symmetry. These have been illuminated in [7]. However, we feel that the existing analysis has a few crucial restrictions. These are as follows.

- The calculation has been done mainly in  $(1 + 1)$  spacetime dimensions.
- The inference in  $(3 + 1)$ -dimensions was drawn based on the analysis in two spacetime dimensions by freezing the two components, transverse to the direction of the atom's motion, of photon momentum.
- The conclusion was drawn by allowing the atom to interact with a single photon.

On the other hand, in reality, our spacetime is  $(3 + 1)$ -dimensional and in principle, there is no control over the direction of the wave vector of the emitted virtual photon. Moreover, an atom always faces a sea of photons, and therefore, single photon analysis is not complete enough to give conclusive evidence.

Hence we feel this apparent symmetry at the quantum level due to symmetry in the relative classical motions between Minkowski and Rindler frames needs to be further thoroughly investigated with care. Another situation can be interesting to check – the symmetry at the quantum level due to the symmetry in relative time progress between two frames. In this regard, one can consider the future and past light cone regions of the Minkowski spacetime and compare it with an observer following the Minkowski coordinates, see [10, 11]. The particle creation observed by a quantum probe confined inside these light cone regions is termed as 'Timelike Unruh Effect' for obvious reasons. In the present work, we are interested in checking whether, in these timelike atomic transitions, one can observe the effects reminiscent of the EEP and WEP. We believe it is of particular interest in the current scenario, as these light cone regions resemble the interior of a Schwarzschild black hole, which is not accessible to an observer sitting outside the black hole. These timelike transitions can also account for an excellent toy model for constructing future experimental set-ups to test semi-classical effects, see [10], and could predict useful phenomena to be checked in analogous systems. Here, we would like to mention that the future and past light cone regions are sometimes also called the expanding and contracting degenerate Kasner universes, see [12]. Therefore, in our manuscript, we will interchangeably use the terms future and past Kasner regions to indicate the future and past light cone regions. In particular, in the future (past) light cone region of the Minkowski spacetime, two static frames can be constructed – one uses the Minkowski frame while the other uses light-cone coordinates. One will be interested in checking whether any true symmetry exists between these frames by comparing two situations – mirror is using Minkowski time while the atom is following a time suitable in the future light cone region and vice-versa. Motivated by these facts, we aim to look into these aspects thoroughly. We re-investigated the Minkowski-Rindler situation thoroughly in a separate paper [13].

In the light cone region, we consider two static frames – one for a quantum system, taken as a two-level atom, and another one for a mirror. For them, we investigate the excitation probability of the atom in two situations.

- Case (*i*): In the first set-up, the mirror synchronizes its clock with Minkowski time while the atom is confined within the future light cone, and thus, the atomic transition is observed with respect to the light cone time. So, the interaction picture is being considered in light cone/Kasner time. Therefore, the atom's vacuum state is not the same as the Minkowski vacuum. Consequently, the atom will be excited by absorbing light cone particles, which from the perspective of the mirror can be described as the emission of *time-accelerated* Minkowski particles.

- Case (ii): A classically equivalent time progress can be put forward, which can mimic Case (i). In this set-up, the atom's clock is synchronized with Minkowski time, and the mirror's frame is the light cone region. The interaction picture is done in Minkowski time coordinate. Here also the atom is excited, but by absorbing the Minkowski particle, which can be described as the emission of time-accelerated light cone particle with respect to the light cone time.

Although both cases can mimic each other's classical time evolution, the question is – whether these timelike quantum transitions bear the same symmetry.

We found that the structures of the single photon transition probabilities apparently carry such symmetry when the analysis is done in  $(1 + 1)$ -spacetime dimensions. However, the situation with all modes of the photon is a little subtle due to the existence of divergences like infrared (IR) and ultraviolet (UV). The situation with a single photon in  $(3 + 1)$ -spacetime dimensions is more nuanced. Although only the thermal factors are symmetric under the exchange of photon and atom frequencies, the complete excitation probabilities are not the same when both these frequencies are taken to be the same. Thus, the latter observation shows considerable disagreement with that in two spacetime dimensions. For all modes, the comparison becomes more subtle. Therefore, we believe that the robustness of this aforesaid symmetry is dependent on the dimensionality of the spacetime. The same situation also arises for the Minkowski-Rindler case, which is discussed thoroughly in our other paper [13].

We also perform an investigation of a similar situation in a black hole spacetime. The Kruskal-Szekeres (KS) coordinate transformations inside a Schwarzschild black hole (BH) event horizon resemble the light cone transformations. In this scenario, the Schwarzschild radial coordinate is timelike inside the horizon, and hence, we choose two frames – one uses the KS frame and the other one (situated in the future KS region, i.e. inside the BH, which is static as the spacelike coordinate, Schwarzschild time, is not changing) is using Schwarzschild coordinates. The atom-mirror set-up is again investigated here in  $(1 + 1)$ -dimensions using Kruskal time and Schwarzschild time interaction pictures, respectively, depending upon the frame of the atom. We find that even in two spacetime dimensions, the transition probabilities do not show the aforesaid symmetry. This, however, does not happen outside the black hole horizon [7] and is also in contrast with  $(1 + 1)$ -dimensional Minkowski-light cone results. Moreover, we find some crucial qualitative similarities between the light cone and the BH scenarios in terms of the thermal factor and a periodic prefactor depending on the position of the static atom (or mirror). We believe these similarities and dissimilarities in atomic transitions between the Schwarzschild interior and Minkowski-light cone regions, as compared to the Rindler-Minkowski and outside BH-KS correspondence, can provide us with crucial insight regarding the effect of spacetime geometry on atomic virtual transitions.

Moreover, in [13], we have seen that though the atomic excitation/de-excitation probabilities between classically equivalent scenarios are not equivalent, the excitation to de-excitation ratios (EDRs) for these scenarios can match. This observation encouraged us to propose EDR as the relevant quantity to study the equivalence principle at the quantum level. However, to get a concrete conclusion in this direction, further investigation is necessary, which motivates us to check whether the same can be verified in our current setup. In fact, the current transitions in the atom are phenomenologically different from the response of an accelerated atom. Therefore, the investigation of EDR in the present scenario is very important in validating our proposal and bolstering its applicability in a different situation. It also acts as a toy model for theoretical tests of various aspects related to the equivalence principle. With this motivation, we investigate the de-excitation probabilities and EDRs in the present scenario. Our observations suggest that though the transition probabilities, either excitation or de-excitation probability, in  $(3 + 1)$  dimensions corresponding to the Minkowski-light cone region are not equal for analogous scenarios, the EDRs are the same when the atomic and field frequencies are equal. We further find the de-excitation probabilities and EDRs corresponding to the Schwarzschild interior case. We observe that the de-excitation probabilities show similar behaviour as the excitation probabilities in terms of quantum equivalence. However, in the near-horizon regime, the EDRs are equal for certain conditions, suggesting that EDRs are more appropriate semiclassical measures when comparing the analogy between different classically analogous scenarios.

We believe the present results are important for illuminating the same in Milne Universe due to the analogy between the geometry of the light cone region and a special scenario in the Friedmann–Lemaître–Robertson–Walker (FLRW) metric [6, 14]. The Milne universe corresponds to an expanding cosmological model, specifically an open universe with nonzero spatial curvature and vanishing spacetime curvature. In a particular choice of coordinates that covers a part of the Milne Universe, the metric is identical to that for the light cone region [14]. Thus, it gives rise to the question of whether a specific quantum effect can be affected by these peculiarities compared to a complete flat spacetime. It should also be noted that there is significant scope for the Milne universe to be imitated in analogous systems [15], which also provides additional relevance for studying quantum effects in it. Furthermore, in de-Sitter spacetime for static observers, we can associate two time frames – one with comoving time and the other one with conformal time. Therefore, these results are also relevant in such situations. All these interconnections make our study in the light cone region of the Minkowski background a crucial arena to look into.

This manuscript is organized in the following manner. In Sec. II, we provide the coordinate transformations

necessary for an observer confined to the light cone regions in a Minkowski background. We recall the definition for the Kruskal coordinates suitable inside the event horizon of a Schwarzschild black hole. In this section, we also elucidate the set-up for investigating the transition probability of a two-level atom. In Sec. III, we investigate the excitation probabilities of these atoms in the presence of an infinite mirror in (1+1) and (3+1) dimensional light cone regions. Subsequently, in Sec. IV, we investigate the excitation of atoms inside the event horizon of a Schwarzschild black hole utilizing the Kruskal coordinates of Sec. II. It is to be noted that in Secs. III and IV, we have two scenarios corresponding to each atom-mirror pair in a certain background. In Sec. V, we study the de-excitation probabilities of the atoms for each of these scenarios and estimate the EDRs. We discuss our observations and specify the resemblance between the scenarios of Secs. III and IV, and provide the concluding remarks in Sec. VI.

## II. COORDINATE TRANSFORMATIONS AND THE SET-UP

In this section, we specify the coordinate transformations suitable for the future and the past light cone regions in a Minkowski background. We also indicate the coordinate transformations for observers accelerated along the positive and the negative  $z$ -directions in a flat background. In particular, these two different accelerated observers will be confined to the regions of the right Rindler wedge ( $RRW$ ) and left Rindler wedge ( $LRW$ ). In this section, we also recall the Kruskal-Szekeres (KS) coordinate transformation suitable for a freely falling observer inside the event horizon of a Schwarzschild black hole. It is to be noted that all of these coordinate transformations will be presented for the (1+1) dimensional scenario, and their representation in (3+1) dimensions follows readily. In this section, we will also present the setup necessary to understand the transition of two-level atoms interacting with the background scalar photon field.

### A. Coordinate transformations

Let us first recall sets of coordinates suitable for the future or the past light cone regions of a (1+1) dimensional Minkowski spacetime (see [12]). In particular, for an observer confined in the future light cone region [10, 11], the coordinate relations are

$$t = \frac{c}{a} e^{a\eta/c} \cosh(a\zeta/c^2); \quad (1a)$$

$$z = \frac{c^2}{a} e^{a\eta/c} \sinh(a\zeta/c^2), \quad (1b)$$

where  $(t, z)$  are the Minkowski coordinates, and  $(\eta, \zeta)$  are the coordinate choice for future light cone ( $FLC$ ). One can notice that the above coordinate transformation is bounded in the future region. This is evident from the constraint  $c^2 t^2 - z^2 = c^4 a^{-2} e^{2a\eta/c}$ , which also indicates  $t > 0$  for the above scenario as  $c/a$  is a positive quantity. At the same time, the coordinates suitable for an observer in the past light cone ( $PLC$ ), are given by

$$t = -\frac{c}{a} e^{a\bar{\eta}/c} \cosh(a\bar{\zeta}/c^2); \quad (2a)$$

$$z = -\frac{c^2}{a} e^{a\bar{\eta}/c} \sinh(a\bar{\zeta}/c^2). \quad (2b)$$

In contrast to the previous case, in this scenario  $t < 0$ , and the coordinate transformation corresponds to an observer confined in the past. We would like to mention that both of these above regions of  $FLC$  and  $PLC$  are depicted in schematic diagrams in Fig. 1. We would also like to highlight the analogy between the geometry of light cone regions and a special scenario of the Friedmann-Lemaître-Robertson-Walker (FLRW) spacetime. This scenario, known as the Milne universe, corresponds to the scale factor given by the coordinate time of the FLRW spacetime, see [6, 16]. Milne universe can correspond to expanding cosmological models with zero spacetime curvature. Actually, the light cone-Minkowski type coordinate description also covers a part of the Milne Universe. Thus, with this analogy, the observations related to light cone regions will be applicable to a part of the Milne Universe as well. As stated earlier, in this section, we would also like to mention the coordinate transformations suitable for observers in uniform acceleration along the positive and the negative  $z$ -directions. In particular, these coordinate transformations corresponding to observers confined to the right and the left Rindler wedges are given by

$$t = \frac{c}{a} e^{a\xi/c^2} \sinh(a\tau/c); \quad z = \frac{c^2}{a} e^{a\xi/c^2} \cosh(a\tau/c) \quad \text{In RRW} \quad (3a)$$

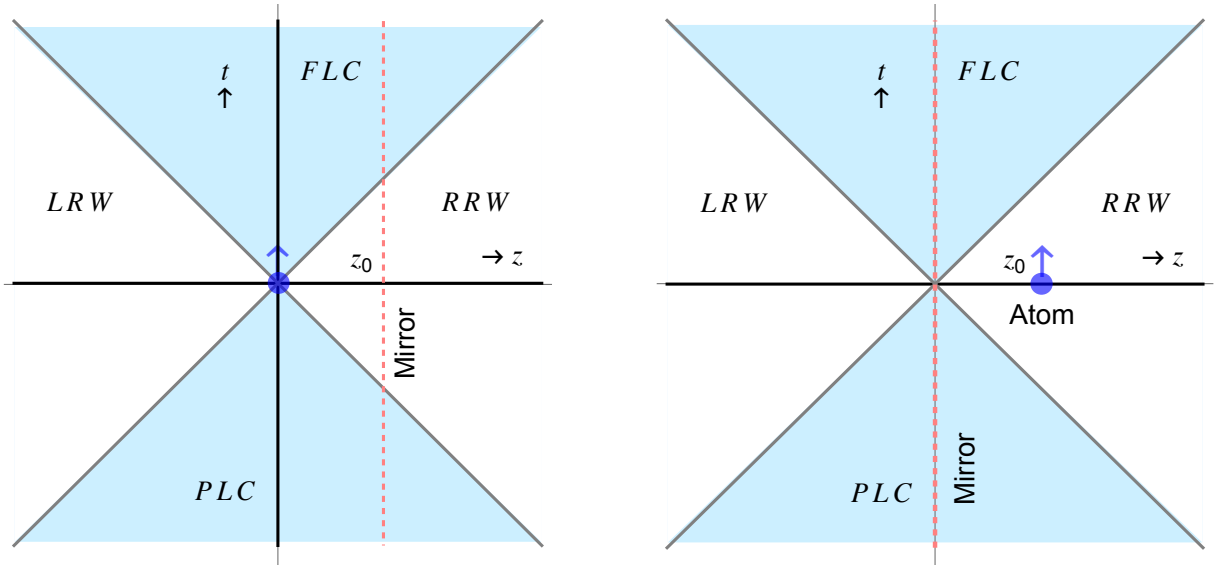


FIG. 1: The above figures provide schematic diagrams depicting different regions in the Minkowski spacetime. The region  $RRW$  denotes the right Rindler wedge, while  $LRW$  denotes the left Rindler wedge. The top and bottom shaded regions, respectively, denote the future and the past light cone regions ( $FLC$  and  $PLC$ ). The above two figures correspond to two different atom and mirror positions. On the left, we have depicted a scenario where the Mirror is kept fixed at  $z = z_0$ , and the atom is in the region  $FLC$  at  $z = 0$ . On the right, the mirror is at  $z = 0$ , and the atom is kept fixed at  $z = z_0$ .

$$t = -\frac{c}{a} e^{a\bar{\xi}/c^2} \sinh(a\bar{\tau}/c); \quad z = -\frac{c^2}{a} e^{a\bar{\xi}/c^2} \cosh(a\bar{\tau}/c) \quad \text{In LRW.} \quad (3b)$$

In the above expression,  $(\tau, \xi)$  and  $(\bar{\tau}, \bar{\xi})$  denote sets of coordinates in the  $RRW$  and  $LRW$ , respectively. A schematic diagram depicting the regions of  $RRW$  and  $LRW$  in a Minkowski background is presented in Fig. 1.

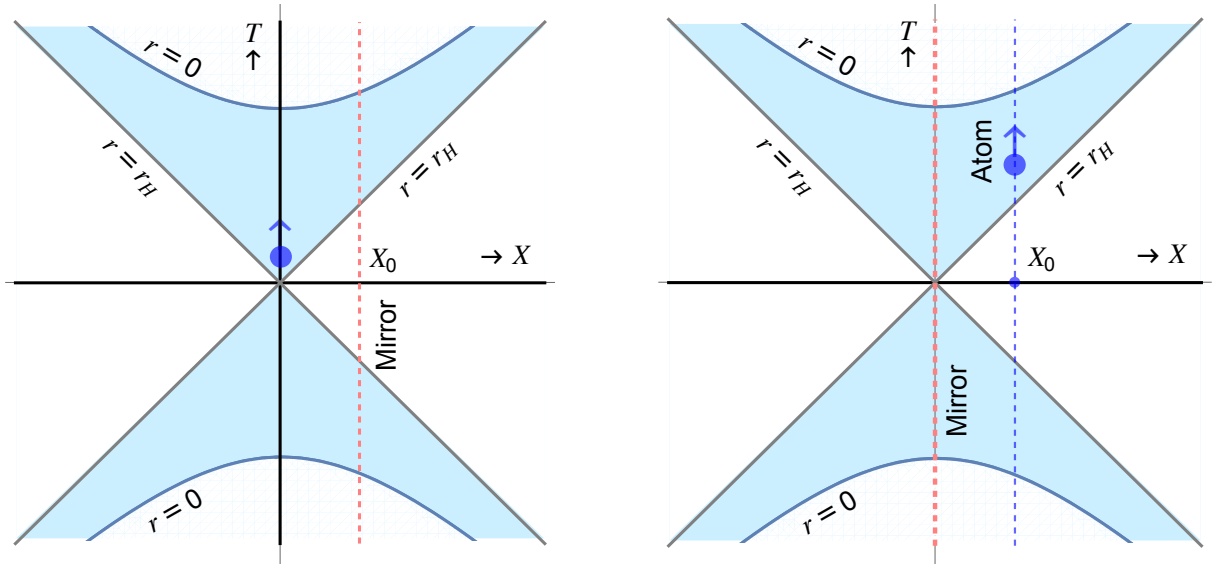


FIG. 2: The above figures provide schematic diagrams depicting the Kruskal-Szekeres representation of the Schwarzschild black hole spacetime. The  $45^\circ$  grey lines denote the event horizon ( $r = r_H$ ). The  $r = 0$  singularity is depicted by curved lines. The shaded regions correspond to the interior of the black hole. The above two figures correspond to two different set-ups for the atom-mirror positions. For instance, on the left, the mirror is free-falling described by a fixed KS space coordinate  $X = X_0$ . In contrast, on the right the atom is free-falling described by  $X = X_0$ .

Next, we consider a Schwarzschild black hole spacetime and we will present the Kruskal coordinate transformation suitable for the region inside its event horizon. In  $(1+1)$  dimensions, the line element in this background, with

coordinates  $(t_S, r)$ , is given by

$$\begin{aligned} ds^2 &= -\left(1 - \frac{r_H}{r}\right) c^2 dt_S^2 + \left(1 - \frac{r_H}{r}\right)^{-1} dr^2 \\ &= \left(1 - \frac{r_H}{r}\right) \left[ -c^2 dt_S^2 + dr_*^2 \right], \end{aligned} \quad (4)$$

where  $r_H$  denotes the position of the event horizon from the central singularity, and  $r_*$  is the tortoise coordinate defined as  $dr_* = (1 - r_H/r)^{-1} dr$ . The KS coordinates suitable for the region inside the black hole, see [17, 18], is given by

$$T = \frac{1}{c\kappa_H} e^{\kappa_H r_*} \cosh(c\kappa_H t_S), \quad X = \frac{1}{\kappa_H} e^{\kappa_H r_*} \sinh(c\kappa_H t_S); \quad (5)$$

where,  $\kappa_H = 1/(2r_H)$  is the surface gravity at the horizon. Furthermore, we consider redefined coordinates inside the black hole, namely the advanced and the retarded time coordinates,  $v = r_* + ct_S$  and  $u = r_* - ct_S$ . Then one can obtain the relation between these coordinates and the KS coordinates as

$$cT + X = \frac{e^{\kappa_H v}}{\kappa_H}; \quad cT - X = \frac{e^{\kappa_H u}}{\kappa_H}. \quad (6)$$

The coordinate transformations mentioned above and the relation between different coordinates will be useful when we estimate the transition probability of atoms in different trajectories in specific regions of the concerned backgrounds. The KS diagram for a Schwarzschild black hole and specifically the black hole interior region in this diagram is depicted in Fig. 2.

## B. Response of atom: the set-up

Here, we elucidate the set-up for investigating the transition probability of electrically neutral atoms. In particular, we consider an atom interacting with a photon field  $\phi$  in the considered background spacetime, be that the light cone region in Minkowski or the future Kruskal region of the Schwarzschild. We consider the atoms to be two-level systems. Depending on different backgrounds and atom trajectories the set-ups to detect the atomic transition will have subtle changes. For instance, when the atom is in the light cone region of the Minkowski spacetime, it is convenient to consider the atomic Hamiltonian to correspond to the conformal time  $\eta$ , see (1), which correctly indicates the dynamical nature of the coordinate transformation described by that region, see [10, 11].

To elucidate on this let us consider an initial atomic state given by  $|\Psi\rangle$  and the Hamiltonian is  $\hat{H} = \hat{H}_0 + \hat{H}_I$ , with  $\hat{H}_0$  and  $\hat{H}_I$  denoting the free and interaction Hamiltonians respectively. In particular, this Hamiltonian is best expressed in terms of the atomic proper time  $\tau$ , i.e., with respect to a clock that is comoving with the atom. This procedure ensures the avoidance of any non-trivial effects due to atomic motion in its energy levels expressed with respect to  $\tau$ . However, a question remains – what will an observer see if it is not comoving with the atom? In that scenario, one needs to understand the change in the Hamiltonian corresponding to that specific trajectory. In particular, the Schrodinger equation with respect to time  $\eta$  will be given by  $i\partial|\Psi\rangle/\partial\eta = (\partial\tau/\partial\eta)\hat{H}|\Psi\rangle$ , see [10]. This motivates us to deduce that with respect to time  $\eta$ , the interaction Hamiltonian is modified by a factor of  $(\partial\tau/\partial\eta)$ . For an atom in the light cone region of the Minkowski spacetime, we consider  $\omega_\eta$  denotes the angular frequency corresponding to the energy gap, which in turn corresponds to the conformal time  $\eta$ , i.e.,  $\omega_\eta$  is obtained from  $i\partial|\Psi\rangle/\partial\eta = (\partial\tau/\partial\eta)\hat{H}|\Psi\rangle$ . From Eq. (1) we observe that  $\partial\tau/\partial\eta = e^{a\eta/c}$  in the future light cone region. Then the interaction Hamiltonian  $\hat{H}_I(\eta)$  corresponding to time  $\eta$  depicting the interaction between the photon and the atom will be given by

$$\hat{H}_I(\eta) = \hbar g e^{a\eta/c} \left( \phi_\nu[t(\eta), z(\eta)] \hat{a}_\nu + h.c. \right) \left( e^{-i\omega_\eta \eta} \hat{\sigma} + h.c. \right). \quad (7)$$

In the above expression,  $\hbar$  is the Planck constant,  $g$  is the atom-field interaction strength,  $\hat{a}_\nu$  is the photon annihilation operator with frequency  $\nu$ ,  $\hat{\sigma}$  is the atomic lowering operator, and  $\phi_\nu$  denotes the photon field mode function. One can notice that the above interaction Hamiltonian is modified by a nontrivial factor  $\partial\tau/\partial\eta = e^{a\eta/c}$ , as compared to its somewhat similar definition with respect to the proper time  $\tau$  [7]. Let the states  $|\omega_0\rangle$  and  $|\omega_1\rangle$  respectively denote the ground and the excited atomic states. We also consider that the field is initially prepared in the vacuum state  $|0\rangle$ . We want to find out the probability for the atom to get excited and simultaneously emit a single photon. In particular, this excitation probability corresponding to the atom of frequency  $\omega_\eta$ , see [7], will be

$$\mathcal{P}_\nu^{ex}(\omega_\eta) = \frac{1}{\hbar^2} \left| \int d\eta \langle 1_\nu, \omega_1 | \hat{H}_I(\eta) | 0, \omega_0 \rangle \right|^2$$

$$= g^2 \left| \int_{-\infty}^{\infty} d\eta e^{a\eta/c} \phi_{\nu}^* [t(\eta), z(\eta)] e^{i\omega_{\eta}\eta} \right|^2. \quad (8)$$

One should note that the above set-up to investigate the transition probability is specific to an atom in the future light cone region of the Minkowski spacetime.

At the same time if the atom is in the Minkowski spacetime the proper time  $\tau$  is given by  $t$ . In this scenario, we consider the atomic angular frequency corresponding to the energy gap to be  $\omega_t$ . Moreover, here the redshift factor is precisely unity. Then the interaction Hamiltonian and the atomic excitation probability can be expressed as

$$\hat{H}_I(t) = \hbar g \left( \phi_{\nu}[t, z] \hat{a}_{\nu} + h.c. \right) \left( e^{-i\omega_t t} \hat{\sigma} + h.c. \right); \quad (9a)$$

$$\mathcal{P}_{\nu}^{ex}(\omega_t) = g^2 \left| \int_{-\infty}^{\infty} dt \phi_{\nu}^* [t, z] e^{i\omega_t t} \right|^2. \quad (9b)$$

It is to be noted that this expression corresponds to an atom that has the proper time  $t$ . This particular set-up was initially proposed in [7] and also used in [19].

Next, if the atom were to be inside the event horizon of the Schwarzschild spacetime, see Eq. (4), the conformal time described by the coordinate  $(r_*/c)$  is appropriate to capture the specific essence of the region. In this scenario, we consider the atomic angular frequency corresponding to the atomic energy gap that is tuned with the conformal time  $(r_*/c)$  to be  $\omega_{r_*}$ . Moreover, we consider  $\tau$  being the proper time in this scenario. Then with the help of Eq. (4) we can find the redshift factor to be  $c\partial\tau/\partial r_* = (-1 + r_H/r)^{1/2}$ . Near the event horizon  $r = r_H$ , this redshift factor can be approximated to be  $c\partial\tau/\partial r_* \simeq e^{r_*/(2r_H)} = e^{\kappa_H r_*}$ . With the help of this redshift factor, one can express the interaction Hamiltonian and the atomic excitation probabilities inside and near the event horizon in an  $(1+1)$  dimensional Schwarzschild black hole spacetime as

$$\hat{H}_I(r_*) = \hbar g c \frac{\partial\tau}{\partial r_*} \left( \phi_{\nu}[t(r_*), z(r_*)] \hat{a}_{\nu} + h.c. \right) \left( e^{-i\omega_{r_*} r_*/c} \hat{\sigma} + h.c. \right); \quad (10a)$$

$$\mathcal{P}_{\nu}^{ex}(\omega_{r_*}) = g^2 \left| \int_{-\infty}^{r_*^f} \frac{dr_*}{c} e^{\kappa_H r_*} \phi_{\nu}^* [t(r_*), z(r_*)] e^{i\omega_{r_*} r_*/c} \right|^2. \quad (10b)$$

We would like to mention that in the above expression, we truncated the integration over  $r_*$  at  $r_*^f$ , as we are interested in observations near the horizon and this expression can be obtained analytically. With the general expression of  $\partial\tau/\partial r_*$ , this integration should have been carried out up to  $r_* = 0$ , which corresponds to the Schwarzschild central singularity. In this second scenario, with general  $\partial\tau/\partial r_*$  inside a black hole, we could not obtain the results analytically, which also contributes to another reason why we chose to obtain the transition probability near the horizon.

On the other hand, with the help of Eqs. (4) and (5) one can notice that the line element in terms of the Kruskal coordinates read as  $ds^2 = (1 - r_H/r) e^{-2\kappa_H r_*} [c^2 dT^2 - dX^2]$ . Thus inside the event horizon of an  $(1+1)$  dimensional Schwarzschild black hole the Kruskal coordinate-time  $T$  and the proper time  $\tau$  are related among themselves as  $\partial\tau/\partial T = (-1 + r_H/r)^{1/2} e^{-\kappa_H r_*}$ . For such an atom following the trajectory described by the Kruskal coordinate transformation (5), the interaction Hamiltonian and the atomic excitation probability are given by

$$\hat{H}_I(T) = \hbar g (\partial\tau/\partial T) \left( \phi_{\nu}[t(T), z(T)] \hat{a}_{\nu} + h.c. \right) \left( e^{-i\omega_T T} \hat{\sigma} + h.c. \right); \quad (11a)$$

$$\mathcal{P}_{\nu}^{ex}(\omega_T) = g^2 \left| \int_{T_-}^{T_+} dT (\partial\tau/\partial T) \phi_{\nu}^* [t(T), z(T)] e^{i\omega_T T} \right|^2. \quad (11b)$$

In the above scenario, we considered the atomic angular frequency to be  $\omega_T$ . In our subsequent analysis, we will see that the integration limits in the above expression  $T_-$  and  $T_+$  are finite as the Kruskal region is bounded by the central singularity and the horizon. It is to be noted that near the event horizon  $r = r_H$  the factor  $\partial\tau/\partial T \simeq 1$ , and with this assumption  $T_{\pm}$  will take certain values. We would like to mention that the above changes are expected to incorporate the essence of the background and the trajectories. It is to be noted that for scalar photons the interaction strength  $g$  is time-independent, see [7], and thus we will treat it as a constant parameter in the estimation of the transition probability. In our subsequent analysis, we shall utilize the above expressions to estimate the transition probability for atoms following different trajectories, and in different background spacetimes. Furthermore, we would like to mention that for the sake of brevity, we shall call all the different atomic angular frequencies  $\omega$  in our subsequent analysis, as their differences in different scenarios are apparent.

### III. ATOMIC EXCITATIONS IN MINKOWSKI-LIGHT CONE REGIONS

In this section, we shall focus on a static atom in the presence of an infinite reflecting static mirror on Minkowski spacetime. However their time progressions are different – one is using Minkowski time while the other one is associated with light cone time and vice versa. We shall consider two distinct scenarios – Case (i) the atom is kept in the region *FLC* at  $\zeta = 0$ , however, its time progression is measured with respect to light cone time  $\eta$ , and the mirror is kept static at  $z = z_0$  whose time frame is given by  $t$ , see Fig. 1; Case (ii) the atom is kept fixed at  $z = z_0$  and so time coordinate is given by  $t$ , while the mirror is in *FLC* at  $\zeta = 0$  and correspondingly time is measured with respect to  $\eta$ , see Fig. 1. We will also consider the (1 + 1) and (3 + 1) dimensional spacetimes separately to investigate and compare the above two scenarios as the spacetime dimensions change.

#### A. (1 + 1) dimensional scenario

Here, we calculate the transition probabilities of the atom from its ground state to its excited state for the above-mentioned Case (i) and Case (ii). In the calculation, whenever necessary, the relations Eq. (1) will be used.

##### 1. Case (i): Static mirror at $z = z_0$

In this scenario, the mirror is static in the Minkowski spacetime and the atom is in the future light cone region and we will study the atomic transition probability with respect to the conformal time  $\eta$ . In this regard, we consider the expression of Eq. (8) for the evaluation of the transition probability. From Eq. (8) it is evident that to investigate the transition probability one needs to find the expression of the photon field mode. The virtual photon is produced in the Mirror's frame, i.e. in Minkowski spacetime. We shall express a single photon mode in (1 + 1) dimensions in the presence of a reflecting mirror. In this regard, we consider the approaches as considered in [6, 7], and obtain

$$\begin{aligned}\phi_\nu &= \frac{1}{\sqrt{4\pi|k|}} \left[ e^{-i\nu t - ik(z-z_0)} - e^{-i\nu t + ik(z-z_0)} \right] \\ &= -\frac{2i \sin\{\nu(z-z_0)/c\}}{\sqrt{4\pi\nu/c}} e^{-i\nu t}.\end{aligned}\quad (12)$$

As we are interested in photon field modes (here taken to be as massless real scalar field), the wave vector and the angular frequency are related as  $\nu = |k|/c$ . This has been utilized in the last equality of Eq. (12). The static atom is in *FLC*, situated at  $z = 0$  (i.e. at  $\zeta = 0$ ). From Eq. (1) we observe that the time relevant for the atom is now  $\eta$ . More precisely the positive frequency modes with respect to the time  $\eta$  corresponds to a conformal vacuum, a state devoid of any particles as seen by an observer with time  $\eta$ . Here the relation among the times along  $\zeta = 0$  is  $t = \frac{c}{a} e^{\frac{a\eta}{c}}$  (see, Eq. (1)). Then in the presence of a mirror, the transition probability of the atom due to the emission of the Minkowski virtual photon will become

$$\begin{aligned}\mathcal{P}_\nu^{ex}(\omega) &= \frac{4g^2c}{4\pi\nu} \left| \int_{-\infty}^{\infty} d\eta e^{a\eta/c} e^{i\nu t} \sin(\nu z_0/c) e^{i\omega\eta} \right|^2 \\ &= \frac{2g^2c^2\omega \sin^2(\nu z_0/c)}{a\nu^3} \frac{1}{e^{2\pi c\omega/a} - 1}.\end{aligned}\quad (13)$$

Now, we would like to mention that one can try to evaluate the transition probability due to the effect of all the field modes by integrating over  $\nu$ , see Appendix A regarding this. In particular, in the current scenario, by integrating over all the modes we get

$$\begin{aligned}\mathcal{P}^{ex}(\omega) &= \frac{2c^2\omega}{a} \frac{1}{e^{2\pi c\omega/a} - 1} \int_{-\infty}^{\infty} dk \frac{g^2 \sin^2(\nu z_0/c)}{\nu^3} \\ &= \frac{2c^2\omega}{a} \frac{1}{e^{2\pi c\omega/a} - 1} \frac{2}{c} \int_0^{\infty} d\nu \frac{g^2 \sin^2(\nu z_0/c)}{\nu^3} = \int_0^{\infty} \mathbb{P}_\nu^{ex}(\omega) d\nu,\end{aligned}\quad (14)$$

where

$$\mathbb{P}_\nu^{ex}(\omega) = \frac{4g^2c\omega}{a} \frac{1}{e^{2\pi c\omega/a} - 1} \frac{\sin^2(\nu z_0/c)}{\nu^3}.\quad (15)$$

It should also be noted that, though the coupling constant  $g$  is independent of  $\tau$ , it is not necessarily independent of the field frequency  $\nu$ , see [7]. The quantity  $\mathbb{P}_\nu^{ex}(\omega)$  is useful as the expression of this quantity can be compared between different scenarios, which will essentially enable one to compare the transition probability for a fixed mode frequency reminiscent of complete probability  $\mathcal{P}^{ex}(\omega)$ . In particular, from the expression (15) we observe that for all well-behaved  $g$  the probability  $\mathbb{P}_\nu^{ex}(\omega)$  is also well-behaved, but it is infrared divergent. This is evident as one takes the limits  $\nu \rightarrow 0$  in expression (15). However, the same might not be true in the ultraviolet limit  $\nu \rightarrow \infty$ , which will be evident if we evaluate the field-independent transition probability, see Eq. (C1) of Appendix C.

## 2. Case (ii): Static atom at $z = z_0$

Here, we consider a static atom at  $z = z_0$  which uses Minkowski clock time  $t$ , and the mirror is at  $z = 0$  (i.e. at  $\zeta = 0$ ) in the region of *FLC*. So, the virtual photons are produced in a mirror frame, which is the light cone region here. Following the procedure presented in [7], we shall decompose the field modes in terms of the coordinates  $(\eta, \zeta)$ , i.e., the coordinates specific to the region *FLC*. Then in  $(1+1)$  dimensions, we have the scalar field mode solution as

$$\phi_\nu(\eta, \zeta) = \frac{1}{\sqrt{4\pi|k|}} \left[ e^{-i\nu\eta + ik\zeta} - e^{-i\nu\eta - ik\zeta} \right]. \quad (16)$$

One should note that with the coordinates specific to the region *PLC* also the above mode function remains the same, with  $(\eta, \zeta)$  replaced by  $(\bar{\eta}, \bar{\zeta})$ . The mirror is fixed at  $z = 0$ , and it corresponds to  $\zeta = 0$ . Moreover, when  $\zeta = 0$  the above field mode vanishes, satisfying the required boundary condition. With the coordinate transformation from Eqs. (1) we have the relations

$$\zeta = \frac{c^2}{a} \tanh^{-1} \left( \frac{z}{ct} \right) \quad , \quad \eta = \frac{c}{2a} \log \left[ \frac{a^2}{c^4} (c^2 t^2 - z^2) \right]. \quad (17)$$

Then one can write down the field mode in terms of the Minkowski coordinates as

$$\phi_\nu(t, z) = \frac{1}{\sqrt{4\pi|k|}} \left( \exp \left\{ \left[ -\frac{i\nu c}{a} \log \left\{ \frac{a}{c^2} (ct - z) \right\} \right] \right\} \Theta(ct - z) - \exp \left\{ \left[ -\frac{i\nu c}{a} \log \left\{ \frac{a}{c^2} (ct + z) \right\} \right] \right\} \Theta(ct + z) \right). \quad (18)$$

In the above the Lorentz-Heaviside  $\Theta$ -function has been introduced. This is because the atom is using Minkowski time which covers  $t \in (-\infty, \infty)$  and therefore it will interact with photon mode, existing both in *FLC* and *PLC* regions. Then the transition probability, with the help of Eq. (9b), for an atom static at  $z = z_0$  will be

$$\begin{aligned} \mathcal{P}_\nu^{ex}(\omega) &= g^2 \left| \int_{-\infty}^{\infty} dt \phi_\nu^*[t, z_0] e^{i\omega t} \right|^2 \\ &= \frac{g^2 c}{4\pi\nu} \left| \int_{z_0/c}^{\infty} dt e^{i\omega t} \left\{ \frac{a}{c^2} (ct - z_0) \right\}^{\frac{i\nu c}{a}} - \int_{-z_0/c}^{\infty} dt e^{i\omega t} \left\{ \frac{a}{c^2} (ct + z_0) \right\}^{\frac{i\nu c}{a}} \right|^2. \end{aligned} \quad (19)$$

We consider a change of variables  $x_1 = ct - z_0$  and  $x_2 = ct + z_0$ . In that scenario, the above integral further simplifies to

$$\begin{aligned} \mathcal{P}_\nu^{ex}(\omega) &= \frac{g^2}{4\pi\nu c} \left| \int_0^\infty dx_1 e^{\frac{i\omega x_1}{c} - \frac{i\omega z_0}{c}} x_1^{\frac{i\nu c}{a}} - \int_0^\infty dx_2 e^{\frac{i\omega x_2}{c} + \frac{i\omega z_0}{c}} x_2^{\frac{i\nu c}{a}} \right|^2 \\ &= \frac{g^2 \sin^2(\omega z_0/c)}{\pi\nu c} \left| \int_0^\infty dx_1 e^{\frac{i\omega x_1}{c}} x_1^{\frac{i\nu c}{a}} \right|^2 \\ &= \frac{2g^2 c^2 \sin^2(\omega z_0/c)}{\omega^2 a} \frac{1}{e^{2\pi c\nu/a} - 1}. \end{aligned} \quad (20)$$

Now we would like to obtain the mode-independent transition probability (see Appendix A) by integrating over the field mode degrees of freedom, i.e., over the wave vector  $k$ . In particular, we obtain this expression as

$$\mathcal{P}^{ex}(\omega) = \frac{4c \sin^2(\omega z_0/c)}{\omega^2 a} \int_0^\infty d\nu \frac{g^2}{e^{2\pi c\nu/a} - 1} = \int_0^\infty \mathbb{P}_\nu^{ex}(\omega) d\nu, \quad (21)$$

where

$$\mathbb{P}_\nu^{ex}(\omega) = \frac{4g^2 c \sin^2(\omega z_0/c)}{\omega^2 a} \frac{1}{e^{2\pi c\nu/a} - 1}. \quad (22)$$

Like earlier, here also  $\mathbb{P}_\nu^{ex}(\omega)$  signifies the transition probability for a fixed mode frequency, reminiscent of a mode independent probability  $\mathcal{P}^{ex}(\omega)$ . For  $g$  to be a well-behaved function of  $\nu$ , as one takes  $\nu \rightarrow 0$ , the above expression in Eq. (22), like Eq. (15), can be seen to be infrared divergent in terms of the field mode frequency.

### B. (3 + 1) dimensional scenario

We now do the same analysis in (3 + 1)-spacetime dimensions. This is a much more realistic situation than the previous (1 + 1)-dimensional analysis as the mirror must be an extended object and in reality we are experiencing (3 + 1) dimension. In (3 + 1) dimensions the coordinate transformations to regions *FLC* and *PLC* remain the same like Eqs. (1) and (2) with the spatial coordinates  $x$  and  $y$  now unchanged. Here also we investigate both situations.

#### 1. Case (i): Static mirror at $z = z_0$

For a static mirror at  $z = z_0$ , i.e., on the  $x - y$  plane, the field modes should be evaluated in terms of the Minkowski coordinates. This field mode solution is straightforward to estimate [6], and is expressed as

$$\begin{aligned} \phi_{\nu, \vec{k}_\perp} &= \frac{1}{\sqrt{(2\pi)^3 2|k|}} e^{-i\nu t + i \vec{k}_\perp \cdot \vec{x}_\perp} \left[ e^{-i k_z (z - z_0)} - e^{i k_z (z - z_0)} \right] \\ &= -\frac{2i \sin\{k_z(z - z_0)\}}{\sqrt{(2\pi)^3 2|k|}} e^{-i\nu t + i \vec{k}_\perp \cdot \vec{x}_\perp}. \end{aligned} \quad (23)$$

In Eq. (23) one can observe that at  $z = z_0$ , i.e., at the position of the mirror, the field mode vanishes. Here also we consider the atom to be static in the future light cone region *FLC* at  $z = 0$ . With this consideration, we use the expression of the above mode solution in Eq. (8) and get the transition probability as

$$\begin{aligned} \mathcal{P}_\nu^{ex}(\omega) &= \frac{4g^2 \sin^2(k_z z_0)}{(2\pi)^3 2|k|} \left| \int_{-\infty}^{\infty} d\eta e^{a\eta/c} e^{i\nu t + i\omega \eta} \right|^2 \\ &= \frac{g^2 c^2 \omega \sin^2(k_z z_0)}{2\pi^2 \nu^3 a} \frac{1}{e^{2\pi c\omega/a} - 1}. \end{aligned} \quad (24)$$

Now we integrate the above expression over the field wave vectors to obtain a field-independent result, like the prescription provided in Appendix A. Then one finds

$$\begin{aligned} \mathcal{P}^{ex}(\omega) &= \frac{c^2 \omega}{2\pi^2 a} \frac{1}{e^{2\pi c\omega/a} - 1} \frac{2\pi}{c^3} \int_0^\infty g^2 \frac{d\nu}{\nu} \int_0^\pi d\theta \sin \theta \sin^2\left(\frac{\nu z_0 \cos \theta}{c}\right) \\ &= \frac{\omega}{\pi a c} \frac{1}{e^{2\pi c\omega/a} - 1} \int_0^\infty g^2 \frac{d\nu}{\nu} \left[ 1 - \frac{c}{2z_0 \nu} \sin\left(\frac{2z_0 \nu}{c}\right) \right] = \int_0^\infty \mathbb{P}_\nu^{ex}(\omega) d\nu. \end{aligned} \quad (25)$$

In the last line, we have carried out the integration over the angle  $\theta$ . In particular, here we have

$$\mathbb{P}_\nu^{ex}(\omega) = \frac{g^2 \omega}{\pi a c} \frac{1}{e^{2\pi c\omega/a} - 1} \left[ 1 - \frac{c}{2z_0 \nu} \sin\left(\frac{2z_0 \nu}{c}\right) \right] \frac{1}{\nu}. \quad (26)$$

From this expression, one can observe that as  $\nu \rightarrow \infty$  the probability  $\mathbb{P}_\nu^{ex}(\omega)$  diverges. Therefore, this probability has an ultraviolet (UV) divergence, unlike the expressions of  $\mathbb{P}_\nu^{ex}(\omega)$  from Eqs. (15) and (22). The origin of this UV divergence can be attributed to the consideration of (3 + 1) dimensions. We would also like to mention that for large  $a$ , especially when  $c\omega/a \ll 1$ , the above expression for transition probability becomes independent of  $a$ . In this scenario, the above transition probability can be approximated to be  $\mathbb{P}_\nu^{ex}(\omega) = g^2 \nu [1 - \sin(z_\nu)/z_\nu] / \{2(\pi c\nu)^2\}$ , where  $z_\nu = 2z_0 \nu/c$ .

2. Case (ii): Static atom at  $z = z_0$

Here we consider the situation where the atom is kept static at  $z = z_0$ , and the mirror is at  $z = 0$  spanning from *PLC* to *FLC*. In  $(3+1)$  dimensional light cone region of Minkowski spacetime, we have the field mode solution, see Appendix B, as

$$\phi_{\nu, \vec{k}_\perp}(\eta, \zeta) = \sqrt{\frac{c^2 \operatorname{cosech}(\pi c \nu / a)}{16\pi^2 a}} J_{-\frac{i c \nu}{a}} \left( \frac{c^2 k_\perp e^{a \eta / c}}{a} \right) e^{\frac{i \nu \zeta}{c} + i \vec{k}_\perp \cdot \vec{x}_\perp}, \quad (27)$$

where  $J_n(x)$  signifies the Bessel function of first kind of order  $n$ , and  $\vec{x}_\perp = (x, y)$  is the spatial distance in the transverse direction. For analytical calculation, we will consider a particular choice of  $a$ . For large  $a$ , one can expand the Bessel function in series as, see [20],

$$J_{-\frac{i c \nu}{a}} \left( \frac{c^2 k_\perp e^{a \eta / c}}{a} \right) \simeq -\frac{i a}{c \nu} \left( \frac{c^2 k_\perp}{2 a} \right)^{-i \nu c / a} \frac{e^{-i \nu \eta}}{\Gamma(i \nu c / a)}. \quad (28)$$

From Eq. (28) one can observe that the field mode of (27) has an outgoing characteristic, as in large  $a$  limit the field mode behaves like  $\phi_{\nu, \vec{k}_\perp}(\eta, \zeta) \sim e^{-i \nu \eta + i \nu \zeta / c}$ . We follow the prescription as provided in [7], according to which the field mode function  $\phi_{\nu, \vec{k}_\perp}(t, z)$  in the atom's frame is obtained from  $\phi_{\nu, \vec{k}_\perp}(t, z) = \{\phi_{\nu, \vec{k}_\perp}(\eta, \zeta) - \phi_{\nu, \vec{k}_\perp}(-\eta, \zeta)\}$  utilizing the coordinate transformation from  $(\eta, \zeta)$  to  $(t, z)$  of Eq. (17). In that scenario,  $\phi_{\nu, \vec{k}_\perp}(t, z)$  will contain both the outgoing and ingoing mode functions. It should also be noted that the outgoing part of this field mode will interact with the atom in the FLC region, i.e., when  $ct > z$ . At the same time, the ingoing part of the mode function will interact with the atom only in the PLC region, i.e., when  $ct > -z$ . Therefore, these outgoing and ingoing parts of the mode functions should be accompanied by the Heaviside step functions  $\Theta(ct - z)$  and  $\Theta(ct + z)$ , respectively (this idea will be used in the latter part of the investigation as well). Then, in the large  $a$  limit, the field mode in the atom's frame can be expressed as

$$\begin{aligned} \phi_{\nu, \vec{k}_\perp}(t, z) &\simeq \sqrt{\frac{c^2 \operatorname{cosech}(\pi c \nu / a)}{16\pi^2 a}} \left( -\frac{i a}{c \nu} \right) \left( \frac{c^2 k_\perp}{2 a} \right)^{-i \nu c / a} \frac{1}{\Gamma(i \nu c / a)} \\ &\times \left( \exp \left\{ \left[ -\frac{i \nu c}{a} \log \left\{ \frac{a}{c^2} (ct - z) \right\} \right] \right\} \Theta(ct - z) \right. \\ &\quad \left. - \exp \left\{ \left[ -\frac{i \nu c}{a} \log \left\{ \frac{a}{c^2} (ct + z) \right\} \right] \right\} \Theta(ct + z) \right). \end{aligned} \quad (29)$$

The transition probability, with the help of Eq. (9b), for the atom static at  $z = z_0$  will be then

$$\begin{aligned} \mathcal{P}_\nu^{ex}(\omega) &= g^2 \left| \int_{-\infty}^{\infty} dt \phi_{\nu, \vec{k}_\perp}^*[t, z_0] e^{i \omega t} \right|^2 \\ &= \frac{g^2 c^2 \operatorname{cosech}(\pi c \nu / a)}{16\pi^2 a} \left( \frac{a^2}{c^2 \nu^2} \right) \frac{1}{|\Gamma(i \nu c / a)|^2} \\ &\times \left| \int_{z_0/c}^{\infty} dt e^{i \omega t} (ct - z_0)^{\frac{i \nu c}{a}} - \int_{-z_0/c}^{\infty} dt e^{i \omega t} (ct + z_0)^{\frac{i \nu c}{a}} \right|^2. \end{aligned} \quad (30)$$

We consider a change of variables  $x_1 = ct - z_0$  and  $x_2 = ct + z_0$ , and proceed in a manner similar to the  $(1+1)$  dimensional case, see Eqs. (19) and (20). Then the above integral becomes

$$\mathcal{P}_\nu^{ex}(\omega) = \frac{g^2 c^2 \sin^2(\omega z_0 / c)}{2 \pi^2 \omega^2 a} \frac{1}{e^{2\pi c \nu / a} - 1}. \quad (31)$$

From the above expression, we can obtain the transition probability for all photon modes by integrating over the field wave vectors. In this regard, we follow the prescription provided in Appendix A. In particular, the field-independent transition probability corresponding to the above expression is obtained as

$$\mathcal{P}^{ex}(\omega) = \frac{c^2 \sin^2(\omega z_0 / c)}{2 \pi^2 \omega^2 a} \frac{4 \pi}{c^3} \int_0^\infty \nu^2 d\nu \frac{g^2}{e^{2\pi c \nu / a} - 1} = \int_0^\infty \mathbb{P}_\nu^{ex}(\omega) d\nu. \quad (32)$$

Here, we have

$$\mathbb{P}_\nu^{ex}(\omega) = \frac{2g^2 \sin^2(\omega z_0/c)}{\pi \omega^2 a c} \frac{\nu^2}{e^{2\pi c \nu/a} - 1}. \quad (33)$$

One can observe that  $\mathbb{P}_\nu^{ex}(\omega)$  is finite in the limit of  $\nu \rightarrow 0$  and  $\nu \rightarrow \infty$  for well-behaved  $g$ . In particular, when  $\nu \rightarrow 0$  the behaviour of the above probability is determined by the numerator  $\nu^2$ , which will result in  $\mathbb{P}_\nu^{ex}(\omega)$  becoming zero. At the same time, when  $\nu \rightarrow \infty$  the behaviour of  $\mathbb{P}_\nu^{ex}(\omega)$  is determined by the denominator, which will again make the quantity zero. These results are in contrast with the one obtained in Eq. (26) corresponding to a static mirror at  $z = z_0$  in  $(3+1)$  dimensions. We would also like to mention that for large  $a$ , more precisely when  $c\nu/a \ll 1$ , the above expression of transition probability simplifies to  $\mathbb{P}_\nu^{ex}(\omega) = g^2 \nu^2 \sin^2[\omega z_0/c]/(\pi \omega c)^2$ .

In this section, we found that due to relative time translation between a two-level atom and a mirror, the virtual photon in one frame creates an atomic transition. It may be noted that classically, the relative time translations between the Minkowski frame and light cone frame are equivalent to those of the respective frames. However, whether this symmetry is still valid in a quantum phenomenon, needs to be investigated. The analysis in  $(1+1)$ -dimensions shows that the transition probabilities (15) and (22) are equal when the photon and atom frequencies are same. Moreover, only the thermal factors for both situations show symmetry under  $\nu \leftrightarrow \omega$ . However, the situation in  $(3+1)$  dimensions is different. Although  $\nu \leftrightarrow \omega$  symmetry exists in thermal factors, but the whole transition probabilities are not the same when one takes  $\nu = \omega$  (see, Eqs. (33) and (26)). It is to be noted that when we take the large  $a$  limit the transition probabilities become independent of  $a$  for both scenarios. However, even at this limit, they do not have a similar functional form. In  $(3+1)$  dimensions, one can identify the origin of this absence of symmetry is the presence of  $k_z$  in Eq. (24). The presence of specific field wave vector  $k_z$  again originates from the directional dependence of quantum transitions on the location of the mirror. On top of that the nature of transition probabilities for all photon modes do not show the same behaviour when compared between two situations, Case (i) and Case (ii). Therefore it seems that the classical symmetry in the relative time translations is not reflected in the atom's transition probabilities when compared between two Killing frames. So the apparent symmetry in two dimensions may be a dimensional artifact.

#### IV. ATOMIC EXCITATIONS FOR BLACK HOLE SPACETIME

In this section, we focus on the atomic transitions under a Schwarzschild black hole spacetime. The inside region of the black hole has a close resemblance with the Minkowski-light cone region when one describes the inside region through KS and Schwarzschild coordinates. Therefore, here, also, we consider two particular scenarios by keeping both atom and mirror fixed at a spatial point. Two timelike coordinates are defined within the BH – one is KS time, and the other one is radial coordinate. Correspondingly two time frames can be associated with mirror and atom, respectively. Two scenarios respectively correspond to – Case (i): atom is static in future KS region on  $X = 0$  (i.e.  $t = 0$ ), and measurement is done using  $r_*/c$  as the time coordinate while the mirror is fixed at  $X_0$  and its time is measured with respect to KS time  $T$ ; Case (ii): here the situation is opposite to Case (i). Our motivation behind considering this particular system is twofold. These two situations are classically identical with respect to the atomic frame. Therefore, like earlier, we want to investigate whether the aforesaid symmetry still holds in the atomic transition. Secondly, the future KS region has an apparent analogy with FLC. Therefore, like RRW and outside BH region correspondence, we want to check whether the transitions in BH have any resemblance with those on Kaner spacetimes. However, from Figs. 1 and 2, it can be seen that the interior of a Schwarzschild black hole is not entirely analogous to the light cone region due to the presence of singularity at  $r = 0$ . Therefore, we expect some modifications in the transition probability compared to the light cone region. We would also like to mention that we will be dealing with a  $(1+1)$  dimensional Schwarzschild black hole spacetime, as in  $(3+1)$  dimensions, the exact functional form of the field mode solution is not known. Moreover, from [21], one can see that though these modes in near-horizon and asymptotic regions become plane wave-like, their behaviour in the  $r \rightarrow 0$  limit is not well defined.

##### A. Case (i): The Mirror is at $X = X_0$

Although both atoms and mirrors are static, their time frame is different. The atom is static at  $X = 0$ , i.e. it is situated on  $t = 0$  axis in Schwarzschild coordinates, and its time frame is measured by  $r_*/c$ . On the other hand, the mirror's time is measured with respect to KS time  $T$ , which is posted at  $X = X_0$ . So, the atom will transit from the ground state to the excited state when encountering the produced virtual photon in the KS frame. Therefore, we describe the photon modes in terms of the KS coordinates, with the vacuum given by the conformal vacuum relating

to the positive frequency mode  $e^{-i\nu T}$ . In particular, this single-photon mode solution, see [6, 7], is given by

$$\phi_\nu = \frac{1}{\sqrt{4\pi|k|}} e^{-i\nu T} \left[ e^{-i|k|(X-X_0)} - e^{i|k|(X-X_0)} \right]. \quad (34)$$

Utilizing this mode solution in the expression of the transition probability of Eq. (10b), we obtain

$$\begin{aligned} \mathcal{P}_\nu^{ex}(\omega) &= \frac{g^2}{4\pi|k|} \left| \int \frac{dr_*}{c} e^{\kappa_H r_*} e^{i\omega r_*/c} e^{i\nu T} \left[ e^{i|k|(X-X_0)} - e^{-i|k|(X-X_0)} \right] \right|^2 \\ &= \frac{g^2 c}{4\pi\nu} \left| \int \frac{dr_*}{c} e^{\kappa_H r_*} e^{i\omega r_*/c} \left[ e^{-i\nu X_0/c} \exp\left\{ \left( \frac{i\nu}{c\kappa_H} e^{\kappa_H v} \right) \right\} - e^{i\nu X_0/c} \exp\left\{ \left( \frac{i\nu}{c\kappa_H} e^{\kappa_H u} \right) \right\} \right] \right|^2. \end{aligned} \quad (35)$$

In the last line of the previous equation, we have used the relation between the Kruskal coordinates  $(T, X)$  and the advanced and retarded times  $(v, u)$  from Eq. (6). From the line element (4) in a Schwarzschild black hole background it is evident that inside the event horizon  $r < r_H$  the coordinate  $r_*$  acts as time, while  $t$  behaves as a spatial coordinate. Therefore, we consider the clock time of measurement to be  $r_*/c$ , and we further consider that the atom is fixed at  $t = 0$ . Then the advanced and retarded time coordinates are related to the  $r_*$  as  $v = r_*$  and  $u = r_*$ . With these considerations, the transition probability of the atom can be estimated to be

$$\begin{aligned} \mathcal{P}_\nu^{ex}(\omega) &= \frac{g^2}{4\pi\nu c} \left| \int_{-\infty}^{r_*^f} dr_* e^{\kappa_H r_*} e^{i\omega r_*/c} e^{-i\nu X_0/c} \exp\left\{ \left( \frac{i\nu}{c\kappa_H} e^{\kappa_H r_*} \right) \right\} \right. \\ &\quad \left. - \int_{-\infty}^{r_*^f} dr_* e^{\kappa_H r_*} e^{i\omega r_*/c} e^{i\nu X_0/c} \exp\left\{ \left( \frac{i\nu}{c\kappa_H} e^{\kappa_H r_*} \right) \right\} \right|^2 \\ &= \frac{g^2 \sin^2(\nu X_0/c)}{\pi\nu c} \left| \int_{-r_*^f}^{\infty} dr_* e^{-\kappa_H r_*} e^{-i\omega r_*/c} \exp\left\{ \left( \frac{i\nu}{c\kappa_H} e^{-\kappa_H r_*} \right) \right\} \right|^2. \end{aligned} \quad (36)$$

In the above expression, we have truncated the limit of the integral till  $r_*^f$  rather than to zero, corresponding to the Schwarzschild inner singularity, as the integral is approximated to give the proper results only in the near horizon region. In the integral of the first line in Eq. (36) if we consider a change of variables  $r_* \rightarrow -r_*$ , we shall get the second line. Considering further a change of variable  $\chi = e^{-\kappa_H r_*}$ , one finds the transition probability as

$$\begin{aligned} \mathcal{P}_\nu^{ex}(\omega) &= \frac{g^2 \sin^2(\nu X_0/c)}{\pi\nu c \kappa_H^2} \left| \int_0^{\chi^f} d\chi \chi^{\frac{i\omega}{\kappa_H c}} e^{\frac{i\nu\chi}{c\kappa_H}} \right|^2 \\ &= \frac{2g^2 \omega \sin^2(\nu X_0/c)}{\nu^3 \kappa_H} \frac{1}{e^{2\pi\omega/(c\kappa_H)} - 1} \left| 1 - \frac{\Gamma\left(\frac{i\omega}{c\kappa_H} + 1, -\frac{i\nu\chi^f}{c\kappa_H}\right)}{\Gamma\left(\frac{i\omega}{c\kappa_H} + 1\right)} \right|^2. \end{aligned} \quad (37)$$

From this last expression (37) one can obtain the expression of mode-independent transition probability by integrating over all field modes, see Appendix A. The expression of this mode-independent transition probability is

$$\mathcal{P}^{ex}(\omega) = \frac{4\omega}{\kappa_H c} \frac{1}{e^{2\pi\omega/(c\kappa_H)} - 1} \int_0^\infty d\nu \frac{g^2 \sin^2(\nu X_0/c)}{\nu^3} \left| 1 - \frac{\Gamma\left(\frac{i\omega}{c\kappa_H} + 1, -\frac{i\nu\chi^f}{c\kappa_H}\right)}{\Gamma\left(\frac{i\omega}{c\kappa_H} + 1\right)} \right|^2 = \int_0^\infty \mathbb{P}_\nu^{ex}(\omega) d\nu, \quad (38)$$

where  $\mathbb{P}_\nu^{ex}(\omega)$  is given by

$$\mathbb{P}_\nu^{ex}(\omega) = \frac{4g^2 \omega \sin^2(\nu X_0/c)}{\nu^3 \kappa_H c} \frac{1}{e^{2\pi\omega/(c\kappa_H)} - 1} \left| 1 - \frac{\Gamma\left(\frac{i\omega}{c\kappa_H} + 1, -\frac{i\nu\chi^f}{c\kappa_H}\right)}{\Gamma\left(\frac{i\omega}{c\kappa_H} + 1\right)} \right|^2. \quad (39)$$

If we consider  $g$  to be independent of  $\nu$ , then the probability  $\mathbb{P}_\nu^{ex}(\omega)$  in the limit of  $\nu \rightarrow 0$  is  $\mathbb{P}_\nu^{ex}(\omega) \sim \nu$ . At the same time, in the limit  $\nu \rightarrow \infty$ , this probability becomes  $\mathbb{P}_\nu^{ex}(\omega) \sim \mathcal{O}(1/\nu^3)$ . Therefore, for well-behaved  $g$ , the transition probability  $\mathbb{P}_\nu^{ex}(\omega)$  in this scenario remains well-behaved.

### B. Case (ii): The atom is at $X = X_0$

Here, we consider the atom is static at  $X = X_0$ , and the observer is using KS time  $T$  to measure. Whole the mirror is now static on  $t = 0$  axis (i.e. at  $X = 0$ ) and using  $r_*/c$  as its coordinate time. So, the atom will encounter the virtual photons produced in the frame described by interior Schwarzschild coordinates. We follow a procedure similar to the one proposed in [7] and obtain the concerned photon mode as

$$\begin{aligned}\phi_\nu(r_*, t) &= \frac{1}{\sqrt{4\pi|k|}} \left[ e^{i\nu u/c} \Theta(cT - X) - e^{i\nu v/c} \Theta(cT + X) \right] \\ &= \frac{1}{\sqrt{4\pi|k|}} \left[ \{\kappa_H(cT - X)\}^{i\nu/(\kappa_H c)} \Theta(cT - X) - \{\kappa_H(cT + X)\}^{i\nu/(\kappa_H c)} \Theta(cT + X) \right].\end{aligned}\quad (40)$$

In the last line of the previous expression, we have used the relation of Eq. (6). The  $\Theta$  functions have been introduced as the atom is using KS time and so both future KS and past KS are accessible to the atom. Then the transition probability of the atom fixed at the KS position  $X = X_0$ , with the help of Eq. (11b), is given by

$$\mathcal{P}_\nu^{ex}(\omega) = \frac{g^2 c}{4\pi\nu} \left| \int dT e^{i\omega T} \left[ \{\kappa_H(cT - X_0)\}^{i\nu/(\kappa_H c)} \Theta(cT - X_0) - \{\kappa_H(cT + X_0)\}^{i\nu/(\kappa_H c)} \Theta(cT + X_0) \right] \right|^2 \quad (41)$$

The atom is fixed at  $X = X_0$ , and we have considered the near-horizon approximation to obtain the above expression of the transition probability. One can note that both past KS and future KS regions are bounded by singularity at  $r = 0$ . Because we considered near-horizon expressions for the transition probability, we further restrict the integrals from the horizon to some  $r_*^f$  rather than exactly to  $r = 0$ . Then one can see that the limits of the integration variable  $T$  in the above expression are from  $T_- = -(T_0/c\kappa_H)$  to  $T_+ = (T_0/c\kappa_H)$ , with  $T_0 = (e^{2\kappa_H r_*^f} + \kappa_H^2 X_0^2)^{1/2}$ . Next, we consider change of variables  $\chi_+ = \kappa_H(cT - X_0)$  and  $\chi_- = \kappa_H(cT + X_0)$ . Then the expression for the transition probability becomes

$$\begin{aligned}\mathcal{P}_\nu^{ex}(\omega) &= \frac{g^2 c}{4\pi\nu} \left| \int_{X_0/c}^{T_+} dT e^{i\omega T} \{\kappa_H(cT - X_0)\}^{i\nu/(\kappa_H c)} - \int_{-X_0/c}^{T_+} dT e^{i\omega T} \{\kappa_H(cT + X_0)\}^{i\nu/(\kappa_H c)} \right|^2 \\ &= \frac{g^2 c}{4\pi\nu} \frac{1}{c^2 \kappa_H^2} \left| \int_0^{T_0 - \kappa_H X_0} d\chi_+ e^{\frac{i\omega\chi_+}{c\kappa_H} + \frac{i\omega X_0}{c}} \chi_+^{\frac{i\nu}{\kappa_H c}} - \int_0^{T_0 + \kappa_H X_0} d\chi_- e^{\frac{i\omega\chi_-}{c\kappa_H} - \frac{i\omega X_0}{c}} \chi_-^{\frac{i\nu}{\kappa_H c}} \right|^2 \\ &= \frac{g^2 c}{4\pi\nu} \frac{1}{c^2 \kappa_H^2} \left| 2i \sin(\omega X_0/c) \int_0^{T_0 - \kappa_H X_0} d\chi_+ e^{\frac{i\omega\chi_+}{c\kappa_H}} \chi_+^{\frac{i\nu}{\kappa_H c}} - \int_{T_0 - \kappa_H X_0}^{T_0 + \kappa_H X_0} d\chi_- e^{\frac{i\omega\chi_-}{c\kappa_H} - \frac{i\omega X_0}{c}} \chi_-^{\frac{i\nu}{\kappa_H c}} \right|^2 \\ &= \frac{2g^2 \sin^2(\omega X_0/c)}{\omega^2 \kappa_H} \frac{1}{e^{\frac{2\pi\nu}{c\kappa_H}} - 1} |1 - \Psi_{Sch}|^2.\end{aligned}\quad (42)$$

In the last expression  $\Psi_{Sch}$  is given by

$$\begin{aligned}\Psi_{Sch} &\equiv \Psi_{Sch}(\omega, \nu) \\ &= \frac{1}{\Gamma\left(1 + \frac{i\nu}{c\kappa_H}\right)} \left[ \Gamma\left(1 + \frac{i\nu}{c\kappa_H}, -\frac{i\omega(T_0 - \kappa_H X_0)}{c\kappa_H}\right) \right. \\ &\quad \left. + \frac{e^{-i\omega X_0/c}}{2i \sin(\omega X_0/c)} \left\{ \Gamma\left(1 + \frac{i\nu}{c\kappa_H}, -\frac{i\omega(T_0 + \kappa_H X_0)}{c\kappa_H}\right) - \Gamma\left(1 + \frac{i\nu}{c\kappa_H}, -\frac{i\omega(T_0 - \kappa_H X_0)}{c\kappa_H}\right) \right\} \right].\end{aligned}\quad (43)$$

Here also the mode-independent transition probability, according to Appendix A, can be expressed as  $\mathcal{P}^{ex}(\omega) = \int_0^\infty \mathbb{P}_\nu^{ex}(\omega) d\nu$ , where  $\mathbb{P}_\nu^{ex}(\omega)$  is now

$$\mathbb{P}_\nu^{ex}(\omega) = \frac{4g^2 \sin^2(\omega X_0/c)}{\omega^2 \kappa_H c} \frac{1}{e^{\frac{2\pi\nu}{c\kappa_H}} - 1} |1 - \Psi_{Sch}|^2. \quad (44)$$

This above quantity in the limit of  $\nu \rightarrow 0$  behaves as  $\mathbb{P}_\nu^{ex}(\omega) \sim g^2/\nu$ , which is divergent if  $g$  is independent of the field frequency; i.e. it contains IR divergence, usually appears in two spacetime dimensions. However,  $\mathbb{P}_\nu^{ex}(\omega)$  remains well behaved in the limit of  $\nu \rightarrow \infty$  if  $g$  is independent of the field frequency  $\nu$ .

Now we like to compare (39) and (44). Note that the thermal factors in both the expressions satisfy the symmetry  $\nu \leftrightarrow \omega$ , whereas the full expressions are not the same when one chooses  $\nu = \omega$ . This contradicts the (1 + 1)-dimensional Minkowski-light cone analysis. Hence the present analysis shows that although from the atom's frame both the cases are equivalent in terms of classical motion, the quantum phenomenon is not. One can notice this disparate feature in the Schwarzschild transition probabilities arrives due to the presence of the terms  $\Gamma[i\omega/(c\kappa_H) + 1, -i\nu\chi^f/(c\kappa_H)]/\Gamma[i\omega/(c\kappa_H) + 1]$  in (39) and  $\Psi_{Sch}$  in (44). Both of these terms will vanish if the interior of the Schwarzschild black hole is not bounded by the finite  $r$  surface and rather if it extends to infinity, which is not possible as even without the near-horizon approximation the radial coordinate is bounded by  $r = 0$  inside the horizon. This observation also makes the present results different from (1 + 1) dimensional Minkowski-light cone results. Therefore, though the trajectories are physically analogous, the interior of a BH compared to the Minkowski-light cone region can lead to interesting differences in terms of quantum signatures. We feel such difference leads to non-equivalence between frames within BH and those in the light cone region, although correspondence between frames in RRW and BH spacetime exists through WEP.

## V. ATOMIC DE-EXCITATIONS AND EXCITATION TO DE-EXCITATION RATIO

In this section, we find the de-excitation probabilities of atoms corresponding to each previously discussed scenario. Subsequently, we also estimate the excitation to de-excitation ratio (EDR) for individual scenarios. It is observed in [13] that even if the individual atomic excitation probabilities corresponding to physically equivalent scenarios are not equivalent, the EDRs can indicate similarity, which in turn can provide crucial physical insights as in a realistic scenario it is more plausible to identify the EDRs corresponding to an atomic system than excitations or de-excitations. This motivated us to investigate the EDRs, also in our current work. In the following few subsections, we shall first estimate the de-excitation probabilities in the light cone and Kruskal regions, and then the EDRs corresponding to each scenario.

### A. Atomic De-Excitation in Minkowski-light cone regions

In this part of the section, we investigate the atomic de-excitations in the light cone region of the Minkowski spacetime. In this regard, we first consider the (1 + 1) dimensional scenario and then the (3 + 1) dimensional scenario. In both dimensions, we shall also consider the situations with either the atom following the light cone time or the mirror following the light cone time.

In particular, with the help of the Hamiltonian defined in Eq. (7) and the analysis from [13] one can obtain the formula of the de-excitation probability corresponding to an atom following the light cone time as

$$\mathcal{P}_\nu^{de}(\omega_\eta) = g^2 \left| \int_{-\infty}^{\infty} d\eta e^{a\eta/c} \phi_\nu^*[t(\eta), z(\eta)] e^{-i\omega_\eta \eta} \right|^2. \quad (45)$$

Similarly, for an atom following the Minkowski time and the mirror following the light cone time, we consider the appropriate Hamiltonian from Eq. (9a). Then with the help of Eq. (9b) and the analysis from [13] we obtain the formula for the de-excitation probability as

$$\mathcal{P}_\nu^{de}(\omega_t) = g^2 \left| \int_{-\infty}^{\infty} dt \phi_\nu^*[t, z] e^{-i\omega_t t} \right|^2. \quad (46)$$

In our following analysis, we shall utilize these two formulas from Eqs. (45) and (46) to obtain the de-excitation probabilities in (1 + 1) and (3 + 1) dimensions respectively.

#### 1. (1 + 1) dimensional scenario

*Case (i): Static mirror at  $z = z_0$  :-* Here, we investigate the scenario in which an atom is static in the light cone region at  $\xi = 0$ , and a mirror is static in Minkowski spacetime at  $z = z_0$ , i.e., the atom the following the Kasner proper time and the field modes are represented in terms of the Minkowski time. Eq. (12) gives the field mode solution for this situation. Combining this field mode solution with equation (45) for the de-excitation probability we obtain

$$\mathcal{P}_\nu^{de}(\omega) = \frac{4g^2c}{4\pi\nu} \left| \int_{-\infty}^{\infty} d\eta e^{a\eta/c} e^{i\nu t} \sin(\nu z_0/c) e^{-i\omega \eta} \right|^2$$

$$= \frac{2g^2 c^2 \omega \sin^2(\nu z_0/c)}{a \nu^3} \frac{1}{1 - e^{-2\pi c \omega/a}}. \quad (47)$$

One can compare this result with the (1 + 1) dimensional result for excitation from Eq. (13), and observe that by making  $\omega \rightarrow -\omega$  in (13) one can obtain the de-excitation result. This is crucial observation which may not hold to be true in other scenarios.

*Case (ii): Static atom at  $z = z_0$  :-* Here, we investigate the case where the atom is static in Minkowski spacetime at  $z = z_0$ , and the mirror is static in the light cone region at  $\xi = 0$ , i.e., the atom is following the Minkowski time and the field modes are represented in terms of the light cone coordinates. The field mode solution for this scenario, obtained in terms of the light cone coordinates and then represented in terms of the Minkowski coordinates, is provided in Eq. (18). Utilizing this field mode solution with the de-excitation probability equation (46), we obtain

$$\begin{aligned} \mathcal{P}_\nu^{de}(\omega) &= g^2 \left| \int_{-\infty}^{\infty} dt \phi_\nu^*[t, z_0] e^{-i\omega t} \right|^2 \\ &= \frac{2g^2 c^2 \sin^2(\omega z_0/c)}{\omega^2 a} \frac{1}{1 - e^{-2\pi c \nu/a}}. \end{aligned} \quad (48)$$

One can observe the significant resemblance of this expression with (1 + 1) dimensional excitation probability from Eq. (20). However, unlike the atom following the light cone time scenario, in this case, one cannot obtain the de-excitation probability by making  $\omega \rightarrow -\omega$  in Eq. (20). This de-excitation probability cannot be obtained by even making  $\nu \rightarrow -\nu$  in the excitation probability expression. We would also like to mention that similar to the excitation probabilities, here also, the de-excitation probabilities corresponding to the two different scenarios from Eqs. (47) and (48) become the same when atomic and field frequencies are equal, i.e., when  $\omega = \nu$ .

## 2. (3 + 1) dimensional scenario

*Case (i): Static mirror at  $z = z_0$ :-* The situation where the mirror is static  $z = z_0$  on the  $x - y$  plane and the atom is static in the future light cone region FLC  $z = 0$  is examined here, i.e., the atom following the light cone time. In this scenario, the field mode solution is provided in Eq. (23). Using this field mode solution and the de-excitation probability formula (45), we obtain

$$\begin{aligned} \mathcal{P}_\nu^{de}(\omega) &= \frac{4g^2 \sin^2(k_z z_0)}{(2\pi)^3 2|k|} \left| \int_{-\infty}^{\infty} d\eta e^{a\eta/c} e^{i\nu t - i\omega \eta} \right|^2 \\ &= \frac{g^2 c^2 \omega \sin^2(k_z z_0)}{2\pi^2 \nu^3 a} \frac{1}{1 - e^{-2\pi c \omega/a}}. \end{aligned} \quad (49)$$

Like the (1 + 1) dimensional scenario, here also one can obtain this de-excitation probability by making  $\omega \rightarrow -\omega$  in the excitation probability expression of Eq. (24). Therefore, in both (1 + 1) and (3 + 1) dimensions, if the atom follows the light cone time, the de-excitation probability can be obtained from the excitation by changing the sign of the atomic energy gap. However, this is not true when the atom is following the Minkowski time and the mirror is in the light cone region.

*Case(ii): Static atom at  $z = z_0$ :-* Here, we examine the scenario where the mirror is at  $z = 0$  spanning from PLC to FLC, and the atom stays stationary at  $z = z_0$ , i.e., the atom is following the Minkowski time and the field modes are realized in terms of the light cone coordinates. In this case, the field mode solution, obtained in terms of the light cone coordinates and then represented in terms of the Minkowski coordinates, is given in Eq. (29). Using this field mode solution along with the expression of the de-excitation probability from equation (46), we obtain

$$\begin{aligned} \mathcal{P}_\nu^{de}(\omega) &= g^2 \left| \int_{-\infty}^{\infty} dt \phi_{\nu, \vec{k}_\perp}^*[t, z_0] e^{-i\omega t} \right|^2 \\ &= \frac{g^2 c^2 \sin^2(\omega z_0/c)}{2\pi^2 \omega^2 a} \frac{1}{1 - e^{-2\pi c \nu/a}}. \end{aligned} \quad (50)$$

Here also, like the (1 + 1) dimensional case, one can see that by making either  $\omega \rightarrow -\omega$  or  $\nu \rightarrow -\nu$  in the expression of the excitation probability (31), one cannot obtain this de-excitation probability. This observation provides additional distinction between the scenarios with the atom following the light cone and Minkowski time. Note that the de-excitation probabilities from Eqs. (49) and (50) are not matching when  $\nu = \omega$ .

A tabular list of our observations			
Dimensions	Excitation/De-excitation	Atom following light cone/ Minkowski time	Transition probabilities $\mathcal{P}_\nu^{ex/de}(\omega)$
(1 + 1)	Excitation	light cone	$\mathcal{P}_\nu^{ex}(\omega) = \frac{2g^2 c^2 \omega \sin^2(\nu z_0/c)}{a \nu^3 e^{2\pi \omega c/a} - 1}$
		Minkowski	$\mathcal{P}_\nu^{ex}(\omega) = \frac{2g^2 c^2 \sin^2(\omega z_0/c)}{a \omega^2 e^{2\pi \nu c/a} - 1}$
	De-excitation	light cone	$\mathcal{P}_\nu^{de}(\omega) = \frac{2g^2 c^2 \omega \sin^2(\nu z_0/c)}{a \nu^3 1 - e^{-2\pi \omega c/a}}$
		Minkowski	$\mathcal{P}_\nu^{de}(\omega) = \frac{2g^2 c^2 \sin^2(\omega z_0/c)}{a \omega^2 1 - e^{-2\pi \nu c/a}}$
(3 + 1)	Excitation	light cone	$\mathcal{P}_\nu^{ex}(\omega) = \frac{g^2 c^2 \omega \sin^2(k_z z_0)}{2\pi^2 \nu^3 a e^{2\pi \omega c/a} - 1}$
		Minkowski	$\mathcal{P}_\nu^{ex}(\omega) = \frac{g^2 c^2 \sin^2(\omega z_0/c)}{2\pi^2 \omega^2 a e^{2\pi \nu c/a} - 1}$
	De-excitation	light cone	$\mathcal{P}_\nu^{de}(\omega) = \frac{g^2 c^2 \omega \sin^2(k_z z_0)}{2\pi^2 \nu^3 a 1 - e^{-2\pi \omega c/a}}$
		Minkowski	$\mathcal{P}_\nu^{de}(\omega) = \frac{g^2 c^2 \sin^2(\omega z_0/c)}{2\pi^2 \omega^2 a 1 - e^{-2\pi \nu c/a}}$

TABLE I: The above table lists our key observations regarding the atomic transitions in the presence of a mirror in light cone regions of (1 + 1) and (3 + 1) dimensional Minkowski spacetime. We have listed both the atomic excitation and de-excitation probabilities from Secs. III and V.

### B. Atomic De-Excitation in Black Hole Spacetime

In this part of the section, we investigate the de-excitation probabilities for atoms in the presence of a mirror in a Schwarzschild black hole spacetime. In particular, here we deal with two specific scenarios. In one case, the atom is static in the Schwarzschild spacetime, and thus it follows the Schwarzschild coordinate time. In another scenario, the atom follows the Kruskal-Szekeres (KS) time and the mirror is static in Schwarzschild coordinates. If the atom is static inside a Schwarzschild black hole, we assume it follows the Schwarzschild coordinate time  $r_*/c$ . Subsequently, we consider the interaction Hamiltonian depicted in Eq. (10a) and follow the adjacent analysis. Then with the help of the analysis as presented in [13] we obtain the formula for estimating the de-excitation probability as

$$\mathcal{P}_\nu^{de}(\omega_{r_*}) = g^2 \left| \int_{-\infty}^{r_*^f} \frac{dr_*}{c} e^{\kappa_H r_*} \phi_\nu^*[t(r_*), z(r_*)] e^{-i\omega_{r_*} r_*/c} \right|^2. \quad (51)$$

At the same time, when the atom is following the Kruskal time and the mirror is static in Schwarzschild coordinates we consider the interaction Hamiltonian from Eq. (11a), and with the help of [13] one can obtain the formula for de-excitation probability as

$$\mathcal{P}_\nu^{de}(\omega_T) = g^2 \left| \int_{T_-}^{T_+} dT (\partial\tau/\partial T) \phi_\nu^*[t(T), z(T)] e^{-i\omega_T T} \right|^2. \quad (52)$$

In our subsequent analysis we shall be using Eqs. (51) and (52) to obtain the explicit expressions of the de-excitation probabilities corresponding to different scenarios.

#### 1. Case(i): The mirror is at $X = X_0$

Here, we examine the case where a mirror is static in Kruskal-Szekeres (KS) coordinates at  $X = X_0$ , i.e., the mirror's time is measured in KS time. Meanwhile, the atom is static at  $t = 0$  in Schwarzschild spacetime, with its time measured by  $r_*/c$ . In this case, the field mode solution in the KS spacetime is given in Eq. (34). Using this field mode solution along with the expression of the de-excitation probability of (51), we get

$$\begin{aligned} \mathcal{P}_\nu^{de}(\omega) &= \frac{g^2}{4\pi|k|} \left| \int \frac{dr_*}{c} e^{\kappa_H r_*} e^{-i\omega r_*/c} e^{i\nu T} \left[ e^{i|k|(X-X_0)} - e^{-i|k|(X-X_0)} \right] \right|^2 \\ &= \frac{2g^2 \omega \sin^2(\nu X_0/c)}{\nu^3 \kappa_H} \frac{1}{1 - e^{-2\pi\omega/(c\kappa_H)}} \left| 1 - \frac{\Gamma\left(\frac{-i\omega}{c\kappa_H} + 1, -\frac{i\nu X^f}{c\kappa_H}\right)}{\Gamma\left(\frac{-i\omega}{c\kappa_H} + 1\right)} \right|^2. \end{aligned} \quad (53)$$

From the above expression, one can observe that this de-excitation probability can be obtained from the excitation probability of Eq. (37) by making  $\omega \rightarrow -\omega$  in it. This observation is similar to the ones from the light cone scenario when the atom follows the light cone time.

## 2. Case(ii): The atom is at $X = X_0$

Here, we look at the situation where the atom is static at  $X = X_0$  and a mirror is at  $t = 0$ , i.e., the atom follows KS time. In this scenario, the field mode solution in terms of the Schwarzschild coordinates and then represented in terms of the Kruskal coordinates is provided in Eq. (40). Utilizing this field mode solution with the expression of the de-excitation probability of Eq. (52), we obtain:

$$\begin{aligned} \mathcal{P}_\nu^{de}(\omega) &= \frac{g^2 c}{4\pi\nu} \left| \int dT e^{-i\omega T} \left[ \{\kappa_H(cT - X_0)\}^{i\nu/(\kappa_H c)} \Theta(cT - X_0) - \{\kappa_H(cT + X_0)\}^{i\nu/(\kappa_H c)} \Theta(cT + X_0) \right] \right|^2 \\ &= \frac{2g^2 \sin^2(\omega X_0/c)}{\omega^2 \kappa_H} \frac{1}{1 - e^{-\frac{2\pi\nu}{c\kappa_H}}} |1 - \chi_{Sch}|^2. \end{aligned} \quad (54)$$

In the last expression  $\chi_{Sch}$  is given by

$$\begin{aligned} \chi_{Sch} &\equiv \chi_{Sch}(\omega, \nu) \\ &= \frac{1}{\Gamma\left(1 + \frac{i\nu}{c\kappa_H}\right)} \left[ \Gamma\left(1 + \frac{i\nu}{c\kappa_H}, \frac{i\omega(T_0 - \kappa_H X_0)}{c\kappa_H}\right) \right. \\ &\quad \left. + \frac{e^{i\omega X_0/c}}{2i \sin(\omega X_0/c)} \left\{ \Gamma\left(1 + \frac{i\nu}{c\kappa_H}, \frac{i\omega(T_0 + \kappa_H X_0)}{c\kappa_H}\right) - \Gamma\left(1 + \frac{i\nu}{c\kappa_H}, \frac{i\omega(T_0 - \kappa_H X_0)}{c\kappa_H}\right) \right\} \right]. \end{aligned} \quad (55)$$

One can notice that the above de-excitation probability cannot be obtained from the excitation probability of a similar situation from Eq. (42) by making the changes of  $\omega \rightarrow -\omega$  or by making  $\nu \rightarrow -\nu$ . Similar to the excitation probabilities the de-excitation probabilities from Eqs. (53) and (54) are not the same when  $\nu = \omega$ .

## C. Excitation to De-excitation Ratio

Usually it is natural to believe that a quantum state  $|\Psi_{in}\rangle$  should be found in a superposition of ground and excited states, i.e.,  $|\Psi_{in}\rangle = C_0 |\omega_0\rangle + C_1 |\omega_1\rangle$  where  $|\omega_0\rangle$  and  $|\omega_1\rangle$  respectively denote the ground and excited states. When this state evolves over time the final state is also expected to be in some superposition of the ground and excited states but with different coefficients. Therefore, for such a state it is more convenient to discuss about the excitation to de-excitation ratio (EDR) to understand its evolution, which is obtained from the ratio of excitation and de-excitation probabilities, i.e., EDR is  $\mathcal{R}_\nu(\omega) = \mathcal{P}_\nu^{ex}(\omega)/\mathcal{P}_\nu^{de}(\omega)$ . Moreover, it may be pointed out that the individual probabilities (excitation as well as de-excitation) are not purely Planckian in nature. In this case the ‘‘effective temperature’’ is proposed to be identified through EDR (e.g. see [22] and references therein). In fact a similar proposal was also given by S. Weinberg in the case of a non-equilibrium system of photons (see e.g. the discussion in Section 6.2 of [23]). So if temperature is a good physical parameter to check the status of EEP, then EDR can be a valuable quantity in this discussion. With this motivation, in this part of the section, we focus on the excitation to de-excitation ratio (EDR).

In (1 + 1) dimensions, when the atom follows light cone time and is static at  $\xi = 0$ , and the mirror is static in Minkowski spacetime at  $z = z_0$ , we take the expressions of  $\mathcal{P}_\nu^{ex}(\omega)$  and  $\mathcal{P}_\nu^{de}(\omega)$  from Eqs. (13) and (47), and get the expression of EDR as

$$\mathcal{R}_\nu(\omega) = e^{-2\pi\omega c/a}. \quad (56)$$

At the same time, in (1 + 1) dimensions when the mirror is static in light cone region at  $\xi = 0$ , and the atom is static in Minkowski spacetime at  $z = z_0$ , we take the expressions of  $\mathcal{P}_\nu^{ex}(\omega)$  and  $\mathcal{P}_\nu^{de}(\omega)$  from Eqs. (20) and (48), and get the expression of EDR as

$$\mathcal{R}_\nu(\omega) = e^{-2\pi\nu c/a}. \quad (57)$$

We can see from the Eqs. (56) and (57) that when the atomic and field frequencies are equal, that is, when  $\omega = \nu$  the EDR in (1 + 1) dimensions for the static atom in Minkowski spacetime is the same as the EDR for the static

atom in light cone region. In  $(3+1)$  dimensions, when the atom is static in FLC at  $\xi = 0$ , and the mirror is static at  $z = z_0$ , we take the expressions of  $\mathcal{P}_\nu^{ex}(\omega)$  and  $\mathcal{P}_\nu^{de}(\omega)$  from Eqs. (24) and (49), and get the expression of EDR, which is the same as Eq. (56). One can also check Table I for all the expressions corresponding to the light cone regions in Minkowski spacetime. At the same time, in  $(3+1)$  dimensions when the mirror is static at  $\xi = 0$ , and the atom is static in Minkowski spacetime at  $z = z_0$ , we take the expressions of  $\mathcal{P}_\nu^{ex}(\omega)$  and  $\mathcal{P}_\nu^{de}(\omega)$  from eqs. (31) and (50), and get the expression of EDR same as Eq. (57). These observations show that the EDR in  $(3+1)$  dimensions for the static atom in Minkowski spacetime is equal to the EDR for the static atom in the light cone region when the atomic and field frequencies are equal, i.e., when  $\omega = \nu$ .

Let us now estimate the excitation to de-excitation ratio for the black hole spacetime. When the atom is static in Schwarzschild spacetime at  $t = 0$ , and the mirror is static in KS spacetime at  $X = X_0$ , we take the expressions of  $\mathcal{P}_\nu^{ex}(\omega)$  and  $\mathcal{P}_\nu^{de}(\omega)$  from Eqs. (37) and (53), and get the expression of EDR as

$$\begin{aligned} \mathcal{R}_\nu(\omega) &= e^{-2\pi\omega/c\kappa_H} \frac{\left| \Gamma\left(\frac{i\omega}{c\kappa_H} + 1\right) - \Gamma\left(\frac{i\omega}{c\kappa_H} + 1, -\frac{i\nu\chi^f}{c\kappa_H}\right) \right|^2}{\left| \Gamma\left(\frac{-i\omega}{c\kappa_H} + 1\right) - \Gamma\left(\frac{-i\omega}{c\kappa_H} + 1, -\frac{i\nu\chi^f}{c\kappa_H}\right) \right|^2} \\ &= e^{-2\pi\omega/c\kappa_H} \frac{\left| \Gamma\left(\frac{i\omega}{c\kappa_H} + 1\right) - \Gamma\left(\frac{i\omega}{c\kappa_H} + 1, -\frac{i\nu\chi^f}{c\kappa_H}\right) \right|^2}{\left| \Gamma\left(\frac{i\omega}{c\kappa_H} + 1\right) - \Gamma\left(\frac{i\omega}{c\kappa_H} + 1, \frac{i\nu\chi^f}{c\kappa_H}\right) \right|^2}. \end{aligned} \quad (58)$$

At the same time, when the mirror is static in Schwarzschild spacetime at  $t = 0$ , and the atom is static in KS spacetime at  $X = X_0$ , we take the expressions of  $\mathcal{P}_\nu^{ex}(\omega)$  and  $\mathcal{P}_\nu^{de}(\omega)$  from Eqs. (42) and (54), and get the expression of EDR as

$$\mathcal{R}_\nu(\omega) = e^{-2\pi\nu/c\kappa_H} \frac{|1 - \Psi_{Sch}|^2}{|1 - \chi_{Sch}|^2}. \quad (59)$$

Now, we consider the near horizon limit, i.e.,  $r \rightarrow r_H$ . In this limit we also have  $r_* \rightarrow -\infty$  and  $T_0 \rightarrow \kappa_H X_0$ . Then using this limit in the expressions of  $\Psi_{Sch}$  and  $\chi_{Sch}$  from Eqs. 43 and 55 we obtain

$$\Psi_{Sch} \simeq \left[ 1 + \frac{e^{-i\omega X_0/c}}{2i \sin(\omega X_0/c)} \left\{ \frac{\Gamma\left(1 + \frac{i\nu}{c\kappa_H}, -\frac{2i\omega X_0}{c}\right)}{\Gamma\left(1 + \frac{i\nu}{c\kappa_H}\right)} - 1 \right\} \right], \quad (60)$$

and

$$\chi_{Sch} \simeq \left[ 1 + \frac{e^{i\omega X_0/c}}{2i \sin(\omega X_0/c)} \left\{ \frac{\Gamma\left(1 + \frac{i\nu}{c\kappa_H}, \frac{2i\omega X_0}{c}\right)}{\Gamma\left(1 + \frac{i\nu}{c\kappa_H}\right)} - 1 \right\} \right]. \quad (61)$$

Substituting these asymptotic expressions of  $\Psi_{Sch}$  and  $\chi_{Sch}$  from Eqs. (60) and (61) in Eq. (59), and simplifying further we obtain

$$\mathcal{R}_\nu(\omega) = e^{-2\pi\nu/c\kappa_H} \frac{\left| \Gamma\left(1 + \frac{i\nu}{c\kappa_H}\right) - \Gamma\left(1 + \frac{i\nu}{c\kappa_H}, -\frac{2i\omega X_0}{c}\right) \right|^2}{\left| \Gamma\left(1 + \frac{i\nu}{c\kappa_H}\right) - \Gamma\left(1 + \frac{i\nu}{c\kappa_H}, \frac{2i\omega X_0}{c}\right) \right|^2}. \quad (62)$$

In the above expressions of Eqs. (58) and (62), the EDRs are obtained for the excitation and de-excitation probabilities in the near-horizon limit. One can notice that under the two conditions: (i)  $\omega = \nu$  and (ii)  $\chi^f = 2X_0\kappa_H$ , the EDRs from Eqs. (58) and (62) become the same. One should also notice that in the near-horizon limit, where  $\chi^f \rightarrow \infty$  maintaining the equivalence between the EDRs requires the atomic position  $X_0$  to be very large, which can be achieved when  $t_S \rightarrow \infty$  as is observed from Eq. (5). We also observe that, unlike the light cone scenarios of Eqs. (56) and (57) the Schwarzschild EDRs do not describe a purely Boltzmann distribution. In this regard, compare these equations with Eqs. (58) and (62).

## VI. OBSERVATIONS & DISCUSSION

Particle creation by an accelerated observer can be perceived in different ways. For instance, an observer in a uniformly accelerated frame sees thermal distribution of particles in the Minkowski vacuum. Similarly, the Rindler

vacuum, observed from the Minkowski frame, is perceived to be particle-creating with a thermal spectrum. It is known that the spectra corresponding to these two scenarios are identical [5, 12], with an interchange of frequency corresponding to either the Minkowski or Rindler modes. An interesting and somewhat similar situation is proposed in [7] to test EEP, where the transition spectrum of a uniformly accelerated atom in the presence of a static reflecting mirror is observed to be analogous to the virtual transition in a static atom in the presence of a uniformly accelerated mirror. Taking inspiration from the equivalence principle, one can also understand that the spectrum for a static atom with a free-falling mirror will be analogous to the transitions in a free-falling atom with a static mirror in a Schwarzschild black hole spacetime [7]. However, all of these predictions consider the  $(1+1)$  dimensional scenario, a  $(3+1)$  dimensional background can provide intriguing deviations.

In the present work, we investigated the similarity between the virtual transitions corresponding to different atom-mirror set-ups in the region of the Minkowski-light cone. We have considered both the  $(1+1)$  and  $(3+1)$  dimensional spacetime scenarios. Here, two specific atom-mirror set-ups are considered. In one scenario, the mirror is kept static at some  $z = z_0$ , and the atom is confined in the future light cone region at  $z = 0$ , see Secs. III A 1 and III B 1. In the other scenario, the atom is kept static at  $z = z_0$ , and the mirror is in the light cone region, see Secs. III A 2 and III B 2. The observations are done with respect to light cone and Minkowski times, respectively. These different atom-mirror set-ups are illustrated in the schematic diagrams of Fig. 1. We observed the transition probabilities to be thermal for both these set-ups and in both  $(1+1)$  and  $(3+1)$  dimensions. For a static mirror at  $z = z_0$ , the thermal factor relates to atomic frequency  $\omega$ , while for a static atom at  $z = z_0$ , it relates to the field frequency  $\nu$ , see Eqs. (15), (26) and (22), (33). In  $(1+1)$  dimensions, the spectra for both the virtual transitions become identical when the atom and the field frequencies are equal, i.e. when  $\omega = \nu$ , see Eqs. (15) and (22). In  $(3+1)$  dimensions this similarity between the virtual transitions is not present when  $\omega = \nu$ , see Eqs. (26) and (33). Here corresponding to a static mirror at  $z = z_0$ , the atomic transition depends on the field-mode wave-vector ( $k_z$ ) along the direction of separation between the mirror and the atom, which results in its dissimilarity with the transition spectra of an atom static at  $z = z_0$ . Therefore, the  $(3+1)$  dimensional scenario not only provides a practical perspective but also gives new physical insight into the picture. However, it should also be noted that though the individual transition probabilities in  $(3+1)$  dimensions do not match when  $\nu = \omega$ , the excitation to de-excitation ratios (EDRs) do match, see Eqs. (56) and (57) and the adjacent discussion. Therefore, it seems that while quantum equivalence is concerned, the EDRs are more suitable for comparison with analogous scenarios. We would also like to mention that for the light cone region, all the EDRs are described by Boltzmann distributions with respect to either  $\omega$  or  $\nu$  depending on whether the atom or the mirror follows the light cone time.

Next, we noticed the similarity between the light cone coordinate transformations from the Minkowski and the Kruskal coordinate transformations from Schwarzschild coordinates. We investigated the characteristics of atomic transitions in the presence of a mirror inside a  $(1+1)$  dimensional Schwarzschild black hole to compare the findings with those of the light cone scenarios. We chose the atom trajectories to mimic the ones from the light cone scenario. For instance, in one scenario the mirror is at fixed KS coordinate  $X_0$ , which resembles a static mirror in a Minkowski background. In another scenario, the atom is fixed at  $X_0$ , i.e., it is analogous to a static atom in the Minkowski background. The observations are done with respect to Schwarzschild and Kruskal times, respectively. The transition probabilities in these scenarios, see Eqs. (39) and (44), have similarities as well as dissimilarity when compared with those of the light cone scenario. We also observed that these two transition probabilities corresponding to the Schwarzschild case are not the same in the limit of  $\omega \rightarrow \nu$ . This is in contrast to the  $(1+1)$  dimensional light cone scenario. Therefore, we end up concluding that even though the exterior of a black hole can mimic an accelerated observer at the quantum level [7] in  $(1+1)$  dimensions, the same is not true for the interior. Here we have seen that the EDRs corresponding to different scenarios are the same but only in the near horizon regime and when  $\omega = \nu$  and  $\chi^f = 2X_0\kappa_H$ . A notable difference compared to the light cone case is that the EDRs corresponding to the Schwarzschild case are not described by purely Boltzmann distributions, see expressions (58) and (62).

In all of the above cases, we observed a particular feature in the transition probabilities, which is distinct compared to the Rindler scenarios of [7]. We observed that for light cone region, the transition probabilities are  $\mathbb{P}_\nu(\omega) \propto \sin^2(\Omega z_0/c)$ , with  $\Omega$  being either the field frequency  $\nu$  or the atom frequency  $\omega$  depending on whether the mirror or the atom is kept static at  $z = z_0$ . At the same time, inside a Schwarzschild black hole, the transition probability is  $\mathbb{P}_\nu(\omega) \propto \sin^2(\Omega X_0/c)$ , where  $\Omega$  corresponds to the field or the atomic frequency depending on whether the mirror or atom is kept fixed at the KS coordinate  $X_0$ . One can notice that like the uniformly accelerating scenario of [7] here also the transition probabilities are periodic with respect to the distance. However, unlike [7] here the transition probabilities vanish periodically with the separation. Whether this feature can be utilized to verify some of these predictions will be interesting to look into.

In our work, another significant insight is obtained in the integrated versions (considering all possible frequencies of modes) of the transition probabilities. In a practical scenario, it is expected that the atomic transition probability should be independent of the field mode frequency as all field modes collectively interact with the atom to result in transition. However, from the field-independent expressions of the transition probabilities of Appendix C, we observe

that not all these expressions give physically sound outcomes. We see that some of these expressions are actually divergent in nature. Depending on whether the mirror or the atom is kept static at  $z = z_0$  in a Minkowski spacetime, and also depending on the spacetime dimensionality the nature of divergence could be different. For instance, when in the light cone region in  $(1 + 1)$  dimensions the divergences are of infrared (IR) type, see Eqs. (C1) and (C2) and the discussions therein. At the same time, in  $(3 + 1)$  when the atom is kept static at  $z = z_0$  the divergence is of ultraviolet (UV) type. In this regard see Eq. (C3) and the related discussion. Whereas, in  $(3 + 1)$  dimensions when the mirror is static at  $z = z_0$ , the transition probability (C4) is not divergent at all. These observations also provide a significant theoretical understanding of the differences between all these scenarios.

Furthermore, we would like to mention that in all these calculations the atom is excited due to the presence of virtual photons in the mirror's frame. This is because the virtual photon is described with respect to Killing time which is different from the atom's Killing time. Since both mirror and atom are static with respect to spatial position while the time coordinates of measurement are different, the atomic transition is completely due to the relative time translation. Hence we call this phenomenon as a timelike transition phenomenon. Moreover in this case the temperature is given by parameters, like  $a/c$  in the Minkowski-light cone case and  $c\kappa_H$  for the BH case, which have the dimension of frequency. Since within the future light cone region and within the BH no observer is allowed to move along  $\eta = \text{constant}$  and  $r = \text{constant}$  trajectories, we do not call these temperatures Unruh and Hawking temperatures, respectively.

Finally, it is known that the temperature due to the Unruh effect, corresponding to a uniformly accelerating observer, is very small for experimentally achievable acceleration scales. For instance, to detect a temperature of one degree Kelvin from the Unruh effect the necessary acceleration is  $10^{21} m/s^2$ . Whereas, a similar temperature, but not physically the same as the Unruh one, can be observed with inertial atoms if they are in the light cone region with  $a/c \sim 100$  GHz, which can be obtained from the scaling of the atomic energy levels, see [10]. This makes it an experimentally more plausible endeavour to look into the atomic transitions in the light cone region. Moreover, there are experimental set-ups that analogues a reflecting mirror [24–28], which can be utilized along with analogue atomic systems [29–31] to construct suitable experimental set-ups in this regard (see [32] for a recent proposal). Therefore, we believe our current work is not only relevant to the fundamental understanding but also provides a significant scope for future experimental verification. We shall follow up on this in our forthcoming investigations. We would also like to mention that though it may become possible to construct a light cone region-like analogous experimental set-up, it is not clear how to make a set-up analogous to the interior of a black hole, let alone to keep an atom static inside it. In this regard, our investigation, with an atom inside a Schwarzschild black hole, will probably remain hypothetical. However, it has an immense theoretical relevance with the light cone region observations due to their certain similarities in atomic transition spectra.

### Acknowledgments

S.B. would like to thank the Science and Engineering Research Board (SERB), Government of India (GoI), for supporting this work through the National Post Doctoral Fellowship (N-PDF, File number: PDF/2022/000428).

### Appendix A: Mode independent transition probability

In this section of the Appendix, we ponder upon the idea of getting a field mode-independent description of the atomic transition probability. In this regard, we consider the atomic motion described by the time  $\mathbb{t}$ . We further consider that in this scenario the proper time  $\tau$  and this specific time  $\mathbb{t}$  are related among themselves as  $d\tau/d\mathbb{t} = \mathcal{R}(\mathbb{t})$ , which also denotes the redshift factor by which the Hamiltonian corresponding to the proper time should be modified. In particular, the interaction Hamiltonian corresponding to time  $\mathbb{t}$  with the field operator  $\Phi(x)$  integrated over all the field modes can be expressed as

$$\hat{H}_I(\mathbb{t}) = \hbar g \mathcal{R}(\mathbb{t}) \Phi[x(\mathbb{t})] (e^{-i\omega \mathbb{t}} \hat{\sigma} + h.c.) , \quad (\text{A1})$$

where the field operator is decomposed in terms of the ladder operators and the field modes  $\phi_k(x)$  as

$$\Phi(x) = \int d^3k [\phi_k(x) \hat{a}_k + \phi_k^*(x) \hat{a}_k^\dagger] . \quad (\text{A2})$$

One can observe that the above interaction Hamiltonian of Eq. (A1) is similar to the interaction Hamiltonian linear in field operator widely used in Unruh-DeWitt detector models [22, 33–40]. One can utilize the interaction Hamiltonian from Eq. (A1) and obtain the mode-independent transition probability as

$$\mathcal{P}^{ex} = g^2 \int d\mathbb{t} \int d\mathbb{t}' e^{i\omega(\mathbb{t}-\mathbb{t}')} \mathcal{R}^*(\mathbb{t}') \mathcal{R}(\mathbb{t}) \langle 0 | \Phi[x'(\mathbb{t}')] \Phi[x(\mathbb{t})] | 0 \rangle$$

$$= g^2 \int d^3 k \left| \int_{-\infty}^{\infty} dt e^{i\omega t} \mathcal{R}(t) \phi_k^*[x(t)] \right|^2. \quad (\text{A3})$$

One can observe that the transition probabilities  $\mathcal{P}_\nu(\omega)$  from Eqs. (8), (9b), (10b), and (11b) and the mode-independent transition probability from the previous Eq. (A3) are related among themselves as  $\mathcal{P} = \int d^3 k \mathcal{P}_\nu(\omega)$ . In the main body of the manuscript, we used this relation to obtain the mode-independent transition probabilities in possible scenarios.

### Appendix B: Field mode solutions in region *FLC* in (3 + 1) dimensions

In this section of the Appendix, we evaluate the normalized field mode solutions in the future light cone region, i.e., in the region *FLC* see Fig. 1, in a (3 + 1) dimensional Minkowski spacetime. The line element in terms of the coordinates of Eq. (1) in *FLC* is given by  $ds^2 = e^{2a\eta/c}(-c^2 d\eta^2 + d\zeta^2) + dx^2 + dy^2$ . For a massless minimally coupled scalar field  $\Phi$  the equation of motion  $\partial_\mu(\sqrt{-g}g^{\mu\nu}\partial_\nu\Phi) = 0$ , in the region *FLC* becomes

$$-\frac{\partial_\eta^2 \Phi}{c} + c \partial_\zeta^2 \Phi + c e^{2a\eta/c} (\partial_x^2 \Phi + \partial_y^2 \Phi) = 0. \quad (\text{B1})$$

From the line element is evident that the metric components are independent of the coordinates  $(\zeta, x, y)$ . Thus the field mode will be plane wave-like with respect to these coordinates, which is also apparent from the equation of motion of Eq. (B1). This motivates us to consider a field mode solution  $\phi_{\nu, k_\perp} \sim R(\eta) e^{i\nu\zeta + i\vec{k}_\perp \cdot \vec{x}_\perp}$ . Substituting this decomposition in the above equation of motion (B1) gives

$$\partial_\eta^2 R + (\nu^2 + c^2 k_\perp^2 e^{2a\eta/c}) R = 0. \quad (\text{B2})$$

One can obtain the solution of this equation in terms of the Bessel function of the first kind. Finally one can express the normalized mode functions as

$$\phi_{\nu, k_\perp} = \sqrt{\frac{c^2 \operatorname{cosech}(\pi c \nu / a)}{16\pi^2 a}} J_{-\frac{i c \nu}{a}} \left( \frac{c^2 k_\perp e^{a\eta/c}}{a} \right) e^{\frac{i\nu\zeta}{c} + i\vec{k}_\perp \cdot \vec{x}_\perp}, \quad (\text{B3})$$

where  $J_n(x)$  denotes the Bessel function of first kind of order  $n$ . In the previous expression  $\vec{x}_\perp = (x, y)$ , denote the transverse directions. We have used the expression of the mode function from Eq. (B3) in investigating the transition probability of two-level atoms.

### Appendix C: Expressions of $\mathcal{P}^{ex}$ in light cone regions

In this section of the appendix, we consider the coupling strength  $g$  between the atom and the field to be constant and estimate the field mode independent transition probability  $\mathcal{P}^{ex}$  by integrating the  $\mathbb{P}_\nu^{ex}$  for the atom-mirror pairs set up in the light cone region.

#### a. Static mirror at $z = z_0$ in (1 + 1) dimensions

First, we consider the situation when the mirror is static at  $z = z_0$  in (1 + 1) dimensions. We take the expression of  $\mathbb{P}_\nu^{ex}$  from Eq. (15) and integrate it over  $\nu$ . We obtain the resulting expression

$$\mathcal{P}^{ex}(\omega) = \frac{4g^2 c \omega}{a} \frac{1}{e^{2\pi c \omega / a} - 1} \frac{z_0^2}{c^2} \left[ Ci \left( \frac{2z_0 \nu}{c} \right) - \frac{\sin^2 \left( \frac{z_0 \nu}{c} \right) + \frac{z_0 \nu}{c} \sin \left( \frac{2z_0 \nu}{c} \right)}{2 \left( \frac{z_0 \nu}{c} \right)^2} \right]_{z_0 \nu / c = 0}^{\infty}. \quad (\text{C1})$$

In the above expression  $Ci(z)$  denotes the cosine integral function. We would like to mention that in the ultraviolet limit of  $\nu \rightarrow \infty$ , the quantity inside the bracket in the above expression vanishes, i.e., the upper limit of the above expression is zero. At the same time, when  $\nu \rightarrow 0$ , the quantity inside the bracket in the above expression diverges out. Therefore, one can conclude that the above transition probability  $\mathcal{P}^{ex}(\omega)$  has infrared (IR) divergence.

b. *Static atom at  $z = z_0$  in  $(1 + 1)$  dimensions*

Second, we consider the situation when the atom is static at  $z = z_0$  in  $(1 + 1)$  dimensions. In this scenario, we consider the expression of  $\mathbb{P}_\nu^{ex}$  from Eq. (22) and integrate over  $\nu$ . This integration without taking limits gives us

$$\mathcal{P}^{ex}(\omega) = \frac{2g^2 \sin^2(\omega z_0/c)}{\pi\omega^2} \left[ \ln \left( 1 - e^{-2\pi\nu c/a} \right) \right]_{\nu c/a=0}^{\infty}. \quad (\text{C2})$$

It is evident that the above expression diverges when  $\nu \rightarrow 0$ , i.e., the transition probability  $\mathcal{P}^{ex}(\omega)$  is infrared (IR) divergent.

c. *Static mirror at  $z = z_0$  in  $(3 + 1)$  dimensions*

Third, we consider a static mirror at  $z = z_0$  in  $(3 + 1)$  dimensions. In this regard, we consider the expression of  $\mathbb{P}_\nu^{ex}$  from eq. (26). After integrating over  $\nu$  we get the field mode independent expression of the transition probability

$$\begin{aligned} \mathcal{P}^{ex}(\omega) &= \frac{g^2 c^2}{2\pi^2 \omega a} \frac{1}{e^{2\pi c\omega/a} - 1} \frac{2\pi}{c^3} \int_0^\infty \nu d\nu \int_0^\pi d\theta \sin\theta \sin^2\left(\frac{\nu z_0 \cos\theta}{c}\right) \\ &= \frac{g^2 \omega}{\pi a c} \frac{1}{e^{2\pi c\omega/a} - 1} \left[ \ln\left(\frac{z_0 \nu}{c}\right) + \frac{\sin\left(\frac{2z_0 \nu}{c}\right)}{z_0 \nu/c} - Ci\left(\frac{2z_0 \nu}{c}\right) \right]_{z_0 \nu/c=0}^{\infty}. \end{aligned} \quad (\text{C3})$$

Here also, in the above expression  $Ci(z)$  denotes the cosine integral function. For  $\nu \rightarrow 0$  the quantity inside the bracket in the above expression becomes finite and is given by  $\{1 - \gamma - \log(2z_0/c)\}$ . At the same time, when  $\nu \rightarrow \infty$ , the expression inside the bracket diverges out, signifying that the transition probability is ultraviolet (UV) divergent. One can notice that in both the  $(1 + 1)$  dimensional scenarios the transition probabilities were IR divergent, but in the current scenario in  $(3 + 1)$  dimensions it is UV divergent.

d. *Static atom at  $z = z_0$  in  $(3 + 1)$  dimensions*

Fourth, we consider the scenario of a static atom at  $z = z_0$  in  $(3 + 1)$  dimensions. We take the relevant expression of  $\mathbb{P}_\nu^{ex}$  from Eq. (33) and integrate over the variable  $\nu$ , which gives

$$\mathcal{P}^{ex}(\omega) = \frac{2g^2 \sin^2(\omega z_0/c)}{\pi\omega^2 a c} \frac{a^3}{4\pi^3 c^3} \zeta(3). \quad (\text{C4})$$

In the above expression  $\zeta(s)$  signifies the Riemann zeta function, and  $\zeta(3) \sim 1.202$  is finite. Therefore, the above expression is finite without any divergences in the IR and UV limit. This is in contrast to the transition probability for a similar atom-mirror set-up from Eq. (C2) corresponding to a  $(1 + 1)$  dimensional scenario.

- 
- [1] T. Padmanabhan, *Quantum Field Theory: The Why, What and How*. Graduate Texts in Physics. Springer, 2016.
- [2] N. Paunkovic and M. Vojinovic, “Equivalence Principle in Classical and Quantum Gravity,” *Universe* **8** no. 11, (2022) 598, [arXiv:2210.00133](https://arxiv.org/abs/2210.00133) [gr-qc].
- [3] F. Pipa, N. Paunković, and M. Vojinović, “Entanglement-induced deviation from the geodesic motion in quantum gravity,” *JCAP* **09** (2019) 057, [arXiv:1801.03207](https://arxiv.org/abs/1801.03207) [gr-qc].
- [4] W. Unruh, “Notes on black hole evaporation,” *Phys.Rev.* **D14** (1976) 870.
- [5] S. Takagi, “Vacuum noise and stress induced by uniform acceleration: Hawking-unruh effect in rindler manifold of arbitrary dimension,” *Progress of Theoretical Physics Supplement* **88** (1986) 1–142, <http://ptps.oxfordjournals.org/content/88/1.full.pdf+html>.
- [6] N. D. Birrell and P. C. W. Davies, *Quantum fields in curved space*. Cambridge Monographs on Mathematical Physics. Cambridge University Press, 1984.
- [7] A. A. Svidzinsky, J. S. Ben-Benjamin, S. A. Fulling, and D. N. Page, “Excitation of an Atom by a Uniformly Accelerated Mirror through Virtual Transitions,” *Phys. Rev. Lett.* **121** no. 7, (2018) 071301.
- [8] W. G. Unruh and R. M. Wald, “What happens when an accelerating observer detects a rindler particle,” *Phys. Rev. D* **29** (Mar, 1984) 1047–1056. <https://link.aps.org/doi/10.1103/PhysRevD.29.1047>.

- [9] S. A. Fulling and J. H. Wilson, “The Equivalence Principle at Work in Radiation from Unaccelerated Atoms and Mirrors,” *Phys. Scripta* **94** no. 1, (2019) 014004, [arXiv:1805.01013 \[quant-ph\]](#).
- [10] S. J. Olson and T. C. Ralph, “Entanglement between the future and past in the quantum vacuum,” *Phys. Rev. Lett.* **106** (2011) 110404, [arXiv:1003.0720 \[quant-ph\]](#).
- [11] J. Q. Quach, T. C. Ralph, and W. J. Munro, “Berry Phase from the Entanglement of Future and Past Light Cones: Detecting the Timelike Unruh Effect,” *Phys. Rev. Lett.* **129** no. 16, (2022) 160401, [arXiv:2112.00898 \[gr-qc\]](#).
- [12] L. C. Crispino, A. Higuchi, and G. E. Matsas, “The Unruh effect and its applications,” *Rev.Mod.Phys.* **80** (2008) 787–838, [arXiv:arXiv:0710.5373 \[gr-qc\]](#).
- [13] P. K. Kumawat, S. Barman, and B. R. Majhi, “Equivalence in virtual transitions between uniformly accelerated and static atoms: from a bird’s eye,” *JCAP* **02** (2025) 046, [arXiv:2410.21051 \[gr-qc\]](#).
- [14] V. Mukhanov, *Physical Foundations of Cosmology*. Physical Foundations of Cosmology. Cambridge University Press, 2005.
- [15] N. Sánchez-Kuntz, A. Parra-López, M. Tolosa-Simeón, T. Haas, and S. Floerchinger, “Scalar quantum fields in cosmologies with 2+1 spacetime dimensions,” *Phys. Rev. D* **105** no. 10, (2022) 105020, [arXiv:2202.10440 \[gr-qc\]](#).
- [16] V. Mukhanov and S. Winitzki, *Introduction to quantum effects in gravity*. Cambridge University Press, 1 ed., 2007.
- [17] T. Padmanabhan, *Gravitation: Foundations and frontiers*. Cambridge University Press, 12, 2014.
- [18] R. Banerjee and B. R. Majhi, “Hawking black body spectrum from tunneling mechanism,” *Phys. Lett. B* **675** (2009) 243–245, [arXiv:0903.0250 \[hep-th\]](#).
- [19] K. Chakraborty and B. R. Majhi, “Detector response along null geodesics in black hole spacetimes and in a Friedmann-Lemaître-Robertson-Walker Universe,” *Phys. Rev. D* **100** no. 4, (2019) 045004, [arXiv:1905.10554 \[gr-qc\]](#).
- [20] “NIST Digital Library of Mathematical Functions.” F. W. J. Olver, A. B. Olde Daalhuis, D. W. Lozier, B. I. Schneider, R. F. Boisvert, C. W. Clark, B. R. Miller and B. V. Saunders, eds.
- [21] S. Barman, G. M. Hossain, and C. Singha, “Exact derivation of the Hawking effect in canonical formulation,” *Phys. Rev. D* **97** no. 2, (2018) 025016, [arXiv:arXiv:1707.03614 \[gr-qc\]](#).
- [22] S. Barman and B. R. Majhi, “Radiative process of two entangled uniformly accelerated atoms in a thermal bath: a possible case of anti-Unruh event,” *JHEP* **03** (2021) 245, [arXiv:arXiv:2101.08186 \[gr-qc\]](#).
- [23] J. Casas-Vázquez and D. Jou, “Temperature in non-equilibrium states: a review of open problems and current proposals,” *Reports on Progress in Physics* **66** no. 11, (Oct, 2003) 1937.
- [24] C. M. Wilson, G. Johansson, A. Pourkabirian, M. Simoen, J. R. Johansson, T. Duty, F. Nori, and P. Delsing, “Observation of the dynamical Casimir effect in a superconducting circuit,” *Nature* **479** (2011) 376–379.
- [25] P. Lähteenmäki, G. S. Paraoanu, J. Hassel, and P. J. Hakonen, “Dynamical Casimir effect in a Josephson metamaterial,” *Proc. Nat. Acad. Sci.* **110** (2013) 4234–4238, [arXiv:1111.5608 \[cond-mat.mes-hall\]](#).
- [26] J. R. Johansson, G. Johansson, C. M. Wilson, and F. Nori, “Dynamical Casimir Effect in a Superconducting Coplanar Waveguide,” *Phys. Rev. Lett.* **103** (2009) 147003, [arXiv:0906.3127 \[cond-mat.supr-con\]](#).
- [27] J. R. Johansson, G. Johansson, C. M. Wilson, and F. Nori, “Dynamical Casimir effect in superconducting microwave circuits,” *Phys. Rev. A* **82** (2010) 052509, [arXiv:1007.1058 \[quant-ph\]](#).
- [28] D. Barman and B. R. Majhi, “Are multiple reflecting boundaries capable of enhancing entanglement harvesting?,” *Phys. Rev. D* **108** no. 8, (2023) 085007, [arXiv:2306.09943 \[gr-qc\]](#).
- [29] M. Aspachs, G. Adesso, and I. Fuentes, “Optimal quantum estimation of the Unruh-Hawking effect,” *Phys.Rev.Lett.* **105** (2010) 151301, [arXiv:arXiv:1007.0389 \[quant-ph\]](#).
- [30] J. Rodriguez-Laguna, L. Tarruell, M. Lewenstein, and A. Celi, “Synthetic Unruh effect in cold atoms,” *Phys. Rev. A* **95** no. 1, (2017) 013627, [arXiv:1606.09505 \[cond-mat.quant-gas\]](#).
- [31] C. Gooding, S. Biermann, S. Erne, J. Louko, W. G. Unruh, J. Schmiedmayer, and S. Weinfurter, “Interferometric Unruh detectors for Bose-Einstein condensates,” *Phys. Rev. Lett.* **125** no. 21, (2020) 213603, [arXiv:2007.07160 \[gr-qc\]](#).
- [32] D. Barman, D. Ghosh, and B. R. Majhi, “Mirror-enhanced acceleration induced geometric phase: towards detection of Unruh effect,” [arXiv:2405.07711 \[quant-ph\]](#).
- [33] D. Barman, S. Barman, and B. R. Majhi, “Role of thermal field in entanglement harvesting between two accelerated Unruh-DeWitt detectors,” *JHEP* **07** (2021) 124, [arXiv:arXiv:2104.11269 \[gr-qc\]](#).
- [34] S. Barman, D. Barman, and B. R. Majhi, “Entanglement harvesting from conformal vacuums between two Unruh-DeWitt detectors moving along null paths,” *JHEP* **09** (2022) 106, [arXiv:arXiv:2112.01308 \[gr-qc\]](#).
- [35] S. Barman, B. R. Majhi, and L. Sriramkumar, “Radiative processes of single and entangled detectors on circular trajectories in (2+1)-dimensional Minkowski spacetime,” *Phys. Rev. D* **109** no. 10, (2024) 105025, [arXiv:2205.01305 \[gr-qc\]](#).
- [36] D. Barman, S. Barman, and B. R. Majhi, “Entanglement harvesting between two inertial Unruh-DeWitt detectors from nonvacuum quantum fluctuations,” *Phys. Rev. D* **106** no. 4, (2022) 045005, [arXiv:arXiv:2205.08505 \[gr-qc\]](#).
- [37] S. Barman and B. R. Majhi, “Optimization of entanglement depends on whether a black hole is extremal,” *Gen. Rel. Grav.* **56** no. 6, (2024) 70, [arXiv:2301.06764 \[gr-qc\]](#).
- [38] S. Barman, I. Chakraborty, and S. Mukherjee, “Entanglement harvesting for different gravitational wave burst profiles with and without memory,” *JHEP* **09** (2023) 180, [arXiv:arXiv:2305.17735 \[gr-qc\]](#).
- [39] H. K, S. Barman, and D. Kothawala, “Universal role of curvature in vacuum entanglement,” *Phys. Rev. D* **109** no. 6, (2024) 065017, [arXiv:2311.15019 \[gr-qc\]](#).
- [40] S. Barman, I. Chakraborty, and S. Mukherjee, “Signatures of gravitational wave memory in the radiative process of entangled quantum probes,” [arXiv:2405.18277 \[gr-qc\]](#).